Pharmacological Research 128 (2018) 1–17

Contents lists available at ScienceDirect

Pharmacological Research

journal homepage: www.elsevier.com/locate/yphrs

Invited Review

Role of RET protein-tyrosine kinase inhibitors in the treatment RET-driven thyroid and lung cancers

Robert Roskoski Jr.[a,*], Abdollah Sadeghi-Nejad[b]

[a] Blue Ridge Institute for Medical Research, 3754 Brevard Road, Suite 116, Box 19, Horse Shoe, NC 28742-8814, United States
[b] Department of Pediatrics, Tufts Medical Center, Tufts University School of Medicine, 800 Washington Street, Boston, MA 02111-1552, United States

ARTICLE INFO

Article history:
Received 21 December 2017
Accepted 21 December 2017
Available online 25 December 2017

Chemical compounds studied in this article:
Alectinib (PubMed CID: 49806720)
Cabozantinib (PubMED CID: 25102847)
Lenvatinib (PubMED CID: 9823820)
Ponatinib (PubMED CID: 24826799
Sorafenib (PubMED CID: 216239)
Sunitinib (PubMED CID: 5329102
Vandetanib (PubMed CID: 3081361)

Keywords:
Catalytic spine
K/E/D/D
Protein kinase inhibitor classification
Protein kinase structure
Regulatory spine
Targeted cancer therapy

ABSTRACT

RET is a transmembrane receptor protein-tyrosine kinase that is required for the development of the nervous system and several other tissues. The mechanism of activation of RET by its glial-cell derived neurotrophic factor (GDNF) ligands differs from that of all other receptor protein-tyrosine kinases owing to the requirement for additional GDNF family receptor-α (GFRα) co-receptors (GFRα1/2/3/4). *RET* point mutations have been reported in multiple endocrine neoplasia (MEN2A, MEN2B) and medullary thyroid carcinoma. In contrast, RET fusion proteins have been reported in papillary thyroid and non-small cell lung adenocarcinomas. More than a dozen fusion partners of RET have been described in papillary thyroid carcinomas, most frequently CCDC6-RET and NCOA4-RET. RET-fusion proteins, commonly KIF5B-RET, have also been found in non-small cell lung cancer (NSCLC). Several drugs targeting RET have been approved by the FDA for the treatment of cancer: (i) cabozantinib and vandetanib for medullary thyroid carcinomas and (ii) lenvatinib and sorafenib for differentiated thyroid cancers. In addition, alectinib and sunitinib are approved for the treatment of other neoplasms. Each of these drugs is a multikinase inhibitor that has activity against RET. Previous X-ray studies indicated that vandetanib binds within the ATP-binding pocket and forms a hydrogen bond with A807 within the RET hinge and it makes hydrophobic contact with L881 of the catalytic spine which occurs in the floor of the adenine-binding pocket. Our molecular modeling studies indicate that the other antagonists bind in a similar fashion. All of these antagonists bind to the active conformation of RET and are therefore classified as type I inhibitors. The drugs also make variable contacts with other residues of the regulatory and catalytic spines. None of these drugs was designed to bind preferentially to RET and it is hypothesized that RET-specific antagonists might produce even better clinical outcomes. Currently the number of new cases of neoplasms bearing *RET* mutations or RET-fusion proteins is estimated to be about 10,000 per year in the United States. This is about the same as the incidence of chronic myelogenous leukemia for which imatinib and second and third generation BCR-Abl non-receptor protein-tyrosine kinase antagonists have proven clinically efficacious and which are commercially successful. These findings warrant the continued development of specific antagonists targeting RET-driven neoplasms.

Contents

1. Overview of RET protein-tyrosine kinase 2
2. Thyroid cancers 2
   2.1. Classification of thyroid cancers 3

Abbreviations: ARTN, artemin; AS, activation segment; CD, cadherin-like domain; CDK, cyclin-dependent protein kinase; CL, catalytic loop; CS or C-spine, catalytic spine; CTT, carboxyterminal tail; EGFR, epidermal growth factor receptor; FGFR, fibroblast growth factor receptor; GDNF, glial-cell derived neurotrophic factor; GFRα, GDNF family receptor-α; GK, gatekeeper; GRL, Gly-rich loop; JM, juxtamembrane segment; KD, kinase domain; KID, kinase insert domain; MEN, multiple endocrine neoplasia; NTRN, neurturin; NSCLC, non-small cell lung cancer; PDGFR, platelet-derived growth factor receptor; PI-3K, phosphatidylinositol 3-kinase; PSPN, persephin; PKA, protein kinase A; PKC, protein kinase C; RS or R-spine, regulatory spine; Sh1, shell residue 1; TM, transmembrane segment; VEGFR, vascular endothelial growth factor receptor.

* Corresponding author.
E-mail addresses: rrj@brimr.org (R. Roskoski Jr.), asadeghi@tuftsmedicalcenter.org (A. Sadeghi-Nejad).

https://doi.org/10.1016/j.phrs.2017.12.021
1043-6618/

2.2. Treatment of thyroid cancers 4
2.3. Driver mutations in thyroid cancers 4
3. RET fusion proteins in lung cancers 5
4. Properties of the RET protein-tyrosine kinase domain 5
4.1. Primary, secondary, and tertiary structures of the human RET catalytic domain 5
4.2. The hydrophobic spines of human RET, VEGFR2, Bruton tyrosine kinase, and murine PKA catalytic domains 8
5. Drugs approved and in clinical trials for the treatment of RET-driven thyroid and lung cancers 8
5.1. Clinical trial summary 8
5.2. Classification of protein kinase-drug complexes 9
5.3. Structures of RET-drug complexes 10
6. RET point mutations 13
7. Clinical outcomes in response to RET inhibitors 13
8. Epilogue 15
Conflict of interest 15
Acknowledgments 15
References 15

1. Overview of RET protein-tyrosine kinase

RET is a transmembrane receptor protein-tyrosine kinase that is required for the normal development of the brain, the peripheral sympathetic and parasympathetic nervous systems, the neuroendocrine thyroid calcitonin producing C-cells, thyroid and lung as well as hematopoietic progenitors and other tissues [1]. This review focuses on the role of RET in the pathogenesis of thyroid and lung cancers and a discussion of the small molecule drugs that target RET in the treatment of these disorders. We will focus on cabozantinib, lenvatinib, sorafenib, and vandetanib, which are RET and multikinase inhibitors that are FDA-approved for the treatment of thyroid cancers. We will also consider (i) alectinib, an ALK/RET antagonist that is approved for the treatment of ALK^+ non-small cell lung cancer (NSCLC), (ii) ponatinib, a multikinase inhibitor approved for the treatment of Philadelphia chromosome positive acute lymphoblastic leukemia (ALL) and chronic myelogenous leukemia (CML), and (iii) sunitinib, a multikinase inhibitor that is approved for the treatment of renal cell carcinoma (RCC), gastrointestinal stromal tumors (GIST), and pancreatic neuroendocrine tumors (pNET) (www.brimr.org/PKI/PKIs.htm).

As reported in 1985, Takahashi et al. transformed murine NIH 3T3 fibroblasts with sonicated human lymphoma DNA [2]. They determined that the transforming sequence encompassed 34 kilobases and was made up of a rearrangement of two normal but unlinked DNA segments. Because this transforming sequence was the product of gene rearrangement during transfection, they named it "REarranged during Transfection," or RET. Ishizaka et al. mapped the human *RET* gene to chromosome 10 (10q11.2) [3]. Durbee et al. subsequently identified RET as the receptor for the glial-cell derived neurotrophic factor (GDNF) [4]. Beside GDNF, this family includes artemin (ARTN), neurturin (NTRN), and persephin (PSPN) [1]. The nearest relatives of the RET receptor protein-tyrosine kinase include FGFR1/2/3/4 and VEGFR1/2/3 [5].

The mechanism of activation of RET by its ligands differs from that of all other receptor protein-tyrosine kinases owing to the requirement for additional GDNF family receptor-α (GFRα) co-receptors (GFRα1/2/3/4) [1]. These co-receptors are tethered to the external plasma membrane by a glycosylphosphatidylinositol linkage and they form binary complexes with the extracellular RET-activating ligands that in turn bind to RET. Members of the GDNF family exist as a homodimer linked by a disulfide bond. The GDNF dimer interacts with two GFRα complexes to form a dimer (a dimer of dimers) that interacts with two RET receptors to form a hexameric complex that consists of two receptors, two co-receptors, and a ligand dimer (Fig. 1). Although there may be some crossover among the ligands and co-receptors, the chief ligand/co-receptor complexes include GDNF/GFRα1, NTRN/GFRα2, ARTN/GFRα3, and PSPN/GFRα4 (Table 1) [1].

In the absence of ligand-mediated stimulation, RET exists in a dormant non-phosphorylated state. Following ligand-mediated stimulation, the RET receptor dimer undergoes *trans*-phosphorylation leading to increased activity. Unlike that of most other receptor protein-tyrosine kinases [6], the activating phosphorylation sites occur outside of the activation segment [7–9]. There are 18 tyrosine residues within the RET intracellular domain (Table 2). Tyr900 and Tyr905 occur within the activation segment, Y660 and Y697 occur within the JM segment, and Y1029/1062/1090/1096 occur in the carboxyterminal tail. Plaza-Menacho et al. reported that Y697 and Y1062 represent early phosphorylation sites while Y900 and Y905 represent late phosphorylation sites [8,9]. These investigators reported that phosphorylation of Y697 within the JM segment plays an important role in enhancing RET activity.

Additional receptor phosphorylation creates docking sites for a variety of proteins that result in intracellular signaling by a plethora of pathways [1,8]. For example, pY752 and pY928 are docking sites that lead to the activation of the JAK-STAT pathway and cell survival (Table 2). pY981 is a docking site that leads to the activation of Src and the PI–3 K/AKT pathway and cell survival while pY1015 leads to the docking of PLCγ and the activation of PKC. pY1062 and pY1096 are docking sites that lead to the activation of the Ras/MAP kinase pathway and cell proliferation along with the PI–3 K/AKT pathway and cell survival as mediated by several docking proteins including Shc1 and Grb2 and Dok1/2/4/5/6. Moreover, the activation segment pY905 is a docking site for Grb7/10 that contributes to the activation of the Ras/MAP kinase cell proliferation pathway [1].

RET pre-mRNA undergoes alternative splicing to yield three protein isoforms: RET9, RET44, and RET51 (Fig. 1) [1]. These differ at the carboxyterminus with 9, 43, and 51 unique C-terminal amino acid residues following codon 1063. Although RET differs in its mode of activation from other protein-tyrosine kinases owing to the requirement for co-receptors, it contains a typical extracellular domain, a transmembrane segment followed by an intracellular juxtamembrane segment, a kinase domain, and a carboxyterminal tail (Fig. 2). The kinase domain contains an insert of 15 residues. The extracellular domain contains four cadherin-like domain (CD1/2/3/4) repeats of about 110 amino acid residues [13] and a cysteine-rich segment of about 150 amino acid residues just proximal to the transmembrane segment. RET is the only receptor protein-tyrosine kinase with cadherin-like domains. An extracellular Ca^{2+}-binding site occurs between CD2 and CD3.

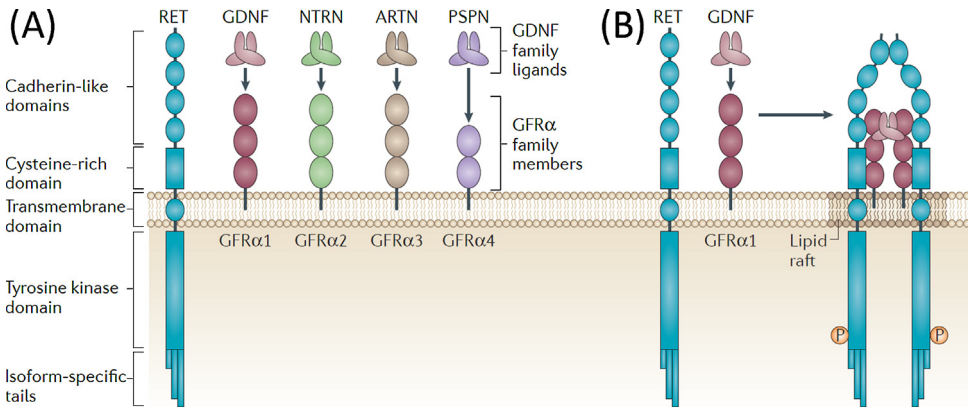

Fig. 1. (A) Activation of the RET receptor protein-tyrosine kinase by its ligands (GDNF, NTRN, ARTN, and PSPN) and its co-receptors (GFRα1/2/3/4). RET has three isoforms that result from alternative splicing of pre-mRNAs leading to the generation of isoform-specific tails. (B) Each RET ligand binds to corresponding co-receptors to form a ligand co-receptor dimer complex that then initiates the formation or RET dimers. Dimerization of RET leads to its activation and the subsequent phosphorylation of residues associated with enzyme activation and the formation of signal transduction docking sites. Reprinted by permission from the Springer Nature Publishing Group Ref. [1] copyright 2014.

Table 1
Properties of the GDNF-GFRα complexes.

Components	UniProtKB IDs	Residues in preproproteins	Residues in mature proteins	Selected functions
GDNF/GFRα1	P39905/P56159	211/465	78–211/25–429	Neuronal development
NTRN/GFRα2	Q99748/O00451	197/464	96–197/22–244	Neuronal development/size of hematopoietic cells
ARTN/GFRα3	Q5T4W7/O60609	220/400	108–220/32–374	Neuronal survival/attracts gut hematopoietic cells
PSPN/GFRα4	O60542/Q9GZZ7	156/299	22–156/21–287	Thyroid C-cell and adrenal medulla development

Table 2
Tyrosine phosphorylation sites.[a]

Residue	Location	Comments[e]
Y660	JM	
Y687[b]	JM	Binds PTPN11 (protein-tyrosine phosphatase non-receptor type 11
Y752[c]	KD, beginning of the β3-strand	Binds STAT3 to activate the JAK/STAT pathway
Y791	KD, beginning of the β4-strand	
Y806[d]	KD, hinge	
Y809[d]	KD, hinge	
Y826[b,c]	KD, KID	
Y864	KD, end of the αE-helix	
Y900[c,d]	KD, AS	
Y905[c,d]	KD, AS	Binds Grb7/10 to activate the Ras/MAP kinase pathway
Y928[c]	KD, substrate binding site	Binds STAT3 to activate the JAK/STAT pathway
Y952	KD, αF-αG loop	
Y981[c,d]	KD, beginning αH-helix	
Y1015[a]	KD, end of KD	Binds PLCγ leading to the activation of PKC
Y1029[b]	CTT	
Y1062[b,d]	CTT	Binds Shc1, FRS2, IRS1/2, Dok1/2/4/5/6, NCK, JNK leading to the activation of PI–3K and RAS/MAP kinase pathways
Y1090[c]	CTT	
Y1096[b,d]	CTT	Binds Grb2, CAB1/2 to activate PI–3K and RAS/MAP kinase pathways

[a] AS, activation segment; CTT, carboxyterminal tail; KD, kinase domain; KID, kinase insert domain; JM, juxtamembrane segment; PLCγ, phospholipase C-γ.
[b] From Ref. [10].
[c] From Ref. [11].
[d] From Ref. [12].
[e] From Ref. [1].

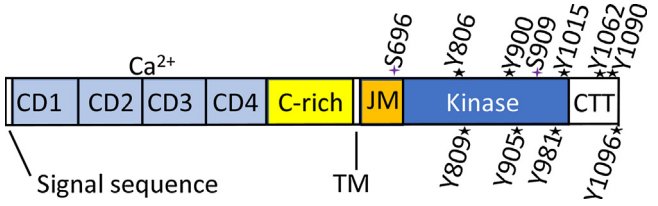

Fig. 2. Overview of the structure of RET receptor protein-tyrosine kinase. Selected serine (S) and tyrosine (Y) phosphorylation sites are depicted. CD, cadherin-like domain; CTT, carboxyterminal tail; JM, juxtamembrane segment; TM, transmembrane segment.

2. Thyroid cancers

2.1. Classification of thyroid cancers

Thyroid carcinoma is the most common endocrine malignancy and accounts for 3–4% of all cancers in the United States (Table 3) [14]. The estimated incidence in 2017 is 57,000 (15,000 male, 42,000 female) with 2000 deaths (900 male, 1100 female). The clinical outcome and survival rates of thyroid neoplasms are markedly better than those of other malignancies [15].

The thyroid gland is primarily made of follicular cells that secrete thyroxine (T4) and to a lesser extent tri-iodothyronine (T3). Differentiated thyroid cancers make up about 93% of thyroid malignancies and they consist of two subtypes: (i) papillary thyroid cancers (PTC) represent about 88% and (ii) follicular thyroid cancers (FTC) represent about 5% of cases. Both of these cancers arise from the thyroid follicular epithelium and their names reflect their histological appearance (papillae or follicles) [15]. Anaplastic thyroid cancers (ATC) are undifferentiated or dedifferentiated tumors that make up about 2% of cases. Medullary thyroid carcinomas make up the remaining 5%. The vast majority of thyroid malignancies (95%) are derived from the follicular epithelium. Exposure to ionizing radiation is a well-known risk factor for papillary thyroid carcinomas [16].

Table 3
Estimated incidence of RET-driven thyroid and lung cancers in 2017.[a]

Classification (% of total)	Incidence	No. (%) with RET mutations or fusion proteins
All thyroid cancers (100%)	57,000	7900 (14%)
Papillary thyroid cancer (84%)	48,000	6200 (11%)
Medullary thyroid cancer (5%)	2800	1700 (60%)
Sporadic medullary thyroid cancer (3.7%)	2100	1050 (50%)
Familial medullary thyroid cancer (1.3%)	700	700 (100%)
NSCLC (100%)	200,000	2000–4000 (1–2%)

[a] Based upon the data in Refs. [16–19].

2.2. Treatment of thyroid cancers

Nearly all patients with thyroid neoplasms present with a mass in the neck [15]. The patient is usually euthyroid clinically and biochemically. Radionuclide scans show a cold nodule (tracer uptake is less than the normal part of the gland). The diagnosis can be established preoperatively by fine needle aspiration.

Total thyroidectomy is the first-line treatment [15]. The extent of surgery depends upon the results of preoperative ultrasound examination of the neck which helps to identify the presence or absence of cervical lymph node involvement. I^{131} is taken up by thyroid follicular cells and, to a lesser degree, by their malignant counterparts. Postoperative scanning permits the identification of residual local foci or distant disease. Since I^{131} is concentrated in thyroid cells, γ-ray emission allows detection and localization of residual thyroid tissue and metastases. Serial measurement of thyroglobulin following surgery is also useful for monitoring the presence/absence of malignant thyroid cells. Undetectable serum thyroglobulin indicates a very low likelihood of residual disease and is a predictor of a better outcome.

Distant metastases occur in about 15% of patients with papillary or follicular thyroid cancer [15]. The most common sites are the lungs and bone, followed by soft tissues. If the site of spread is accessible and localized, surgery is the treatment of choice. In patients with unresectable disease or distant metastases, a therapeutic dose of I^{131} is a treatment option. Here, β-rays induce radiation toxicity and cell death. Moreover, total ablation of thyroid follicular cells (both normal and cancerous) improves the value of measurements of serum thyroglobulin as a marker of recurrent or metastatic disease. Patients with papillary thyroid carcinoma have an excellent prognosis with a 10-year survival of greater than 95%.

Patients with follicular carcinoma also present with a slowly enlarging painless thyroid nodule, but metastases to bone, lungs, or liver are more common than in patients with papillary thyroid carcinomas [15]. The treatment for both disorders is the same, but the prognosis is less favorable for patients with follicular carcinoma. In this group the 10-year survival approaches 50% for patients with metastases and greater than 90% in those without metastases.

Patients with anaplastic thyroid cancer present with a rapidly enlarging neck mass often with symptoms of cough, dysphagia, dyspnea, or hoarseness caused by spread to the recurrent laryngeal nerve [15]. Therapeutic results, thus far, have been disappointing. Treatment is palliative in nature owing to the aggressiveness of the malignancy. For those rare occasions without distant metastases at the time of diagnosis, surgery is recommended as the first-line treatment. Death generally occurs within one year after diagnosis with a mean survival of only six months [16].

Medullary carcinoma of thyroid is distinct from other thyroid neoplasms both clinically and embryologically [15]. Medullary carcinoma results from the malignant transformation of parafollicular thyroid C-cells. These cells, which secret calcitonin and are of neuroendocrine origin, are located in the connective tissue adjacent to thyroid follicles. About 75% of medullary carcinomas are sporadic and 25% are familial in nature and are transmitted as an autosomal dominant trait (Table 3) [20]. Familial medullary thyroid carcinoma usually occurs as a part of a multiple endocrine neoplasia syndrome (80% MEN2A and 5% MEN2B). The other 15% are not associated with other endocrine gland abnormalities [19]. In MEN2A, usually diagnosed in second or third decade, medullary thyroid cancer is associated with pheochromocytoma (50% of cases) and hyperparathyroidism (20–30%). In MEN2B, medullary thyroid cancer may occur within the first year of life and is associated with pheochromocytoma in 50% of patients. These patients may also have mucosal neuromas, intestinal ganglioneuromas, and marfanoid phenotypic features (long limbs, long fingers and toes, and crowded oral maxilla). Medullary carcinomas arising in the context of MEN2B are generally more aggressive than those occurring in MEN2A. In the former (MEN2B) metastatic disease may be present in the first year of life. The malignancy is least aggressive in patients with isolated familial medullary thyroid carcinoma unrelated to MEN2A or MEN2B [19].

Patients with sporadic medullary thyroid carcinoma have a clinically mild disease [15]. Many of these patients are diagnosed following genetic testing of first degree relatives of a patient known to have this malignancy. In other instances, a *de novo* mutation results in a familial index case of medullary thyroid cancer. In the absence of a familial index case, patients present with cardiovascular symptoms related to pheochromocytomas or hypercalcemia due to parathyroid adenomas.

Surgical excision is the first line of therapy in medullary thyroid carcinoma and is curative. [15]. Total thyroidectomy, early in childhood or at diagnosis, is also recommended for asymptomatic carriers. Historically, treatment of patients with inaccessible distant metastases has been difficult and unsatisfactory. There is no role for I^{131} treatment in patients with medullary thyroid cancer because C-cells fail to take up iodine.

2.3. Driver mutations in thyroid cancers

RET point mutations occur in about one half of sporadic (non-familial) medullary thyroid cancers. *RET* point mutations have also been reported in familial medullary thyroid carcinomas and multiple endocrine neoplasia (MEN2A and MEN2B) [1,8,21–24]. In contrast, RET fusion proteins have been reported in papillary thyroid carcinoma and also in non-small cell lung adenocarcinoma as described in Section 3 [1,8,16–18,24–28].

Most papillary thyroid carcinomas have mutations involving the genes encoding the B-Raf protein-serine/threonine kinase, K-Ras, RET, NTRK, or ALK protein-tyrosine kinases [16]. The mutations are mutually exclusive. About one-third of these cancers possess a $BRAF^{V600E}$ gain-of-function mutation (which is associated with extrathyroidal extension and metastatic disease) [18]. Paracentric inversion or translocations of *NTRK1* on chromosome 1q21, which result in enzyme activation, are present in 5–10% of papillary thyroid malignancies. Under physiologic conditions, the *RET* gene product is not expressed in thyroid follicular cells. In papillary cancers, however, a reciprocal translocation between chromosomes 10 and 17 or a paracentric inversion within chromosome 10 places the protein-tyrosine kinase domain under the transcriptional control of genes that are normally expressed within the

thyroid epithelium. More than a dozen fusion partners of RET have been described in papillary thyroid carcinomas including CCDC6, PRKAR1A, NCOA4, GOLGA5, TRIM24, TRIM33, ELKS, KTN1, RFG9, PCM1, TRIM27, HOOK3, ERC1, AKAP13, TBL1XR1, FKBP, SPECC1L, ANK3, and ACBD5 [18,20,24]. Of these, the most commonly identified RET fusions in papillary thyroid carcinomas are CCDC6-RET and NCOA4-RET.

In contrast to papillary neoplasms, follicular carcinomas contain activating mutations of *KRAS* or activating mutations of the PI–3K/AKT pathway [16]. Patients with this disorder present with slowly enlarging painless thyroid nodules; metastases to bone, lungs, or liver are common. Anaplastic thyroid carcinomas contain a variety of molecular alterations including *BRAF, RAS,* or *TERT* promoter mutations, effectors of the PI–3K/AKT pathway, or inactivation of the *TP53* gene [16].

Distant metastases to lung, bone and soft tissue occur in about 15% of patients with papillary or follicular thyroid cancer [15]. In patients with nonresectable disease or distant metastases, I^{131} is a treatment option provided that malignant cells take up the isotope. In patients with progressive disease that does not respond to standard therapies, the use of sorafenib and lenvatinib has been approved by FDA (www.brimr.org/PKI/PKIs.htm) [16]. Sorafenib and lenvatinib are multikinase inhibitors that target RET, VEGFR1/2/3, PDGFRα/β, and Kit. The interaction of these drugs with the RET protein kinase domain is described in Section 5.3.

As discussed previously, surgery is also the mainstay of treatment for both familial and sporadic medullary thyroid carcinomas [15]. For carriers of familial RET mutations associated with severe medullary thyroid carcinomas (codon 609, 611, 618, 620, 630, 634), prophylactic total thyroidectomy is performed at the time of diagnosis. These mutations occur within the cysteine-rich extracellular domain of RET (Fig. 2). For patients with *MEN2B* mutations in codon 883, 918, or V804M/E805K, V804M/Y806C, V804M/S904C double mutations, prophylactic thyroidectomy should be performed in the first year of life. Thyroidectomy can be delayed in patients with less lethal medullary thyroid cancer with mutations involving RET codon 769, 790, 791, 804, or 891, who have surgical contraindications as long as stringent criteria are met and there is close monitoring and follow-up. The use of cabozantinib has been FDA-approved for the treatment of progressive medullary thyroid carcinoma and vandetanib has been approved for the treatment of indolent and progressive medullary thyroid carcinoma (www.brimr.org/PKI/PKIs.htm) [16].

3. RET fusion proteins in lung cancers

Lung cancer accounts for about 13% of all new neoplasms diagnosed in the United States [14]. Siegel et al. estimate that 222,000 people will develop cancer of the lung and bronchus in the United States in 2017 (105,000 women, 117,000 men) and 156,000 people will die of the disease (71,000 women, 85,000 men) [14].

Patients with non-small cell lung cancer often have early metastases. As such they may not be candidates for surgical resection or radiation therapy. Accordingly, chemotherapy is usually the treatment of choice for this group. However, the choice of surgical resection and radiation as the primary therapy in NSCLC is dependent on the patient's general health, the extent of neoplastic involvement, and the presence/absence of co-morbidities. Shaw et al. estimate that 1–2% of patients with NSCLC harbor RET-fusion proteins [18]. With the estimated 222,000 patients developing lung cancer in the US in 2017 and assuming that 90% of these new cases are NSCLC (200,000), the incidence of new cases of RET-fusion protein lung cancer is 2000–4000 per year (Table 3) As a comparison it should be noted that the incidence of new cases of chronic myelogenous leukemia in the same period is thought to be around 9000.

KIF5B-RET is the most common RET fusion partner identified in NSCLC [24]. Other RET fusion partners including CCDC6, NCOA4, and TRIM33 occur in both lung cancer and papillary thyroid cancer [18]. Lung cancer patients with RET-fusion proteins tend to be relatively young (<60 years of age) and have minimal or no prior history of cigarette smoking [24]. Several RET inhibitors that also target other protein kinases are in clinical trials for the treatment of RET-fusion protein positive lung cancer including cabozantinib, vandetanib, ponatinib, sunitinib, and sorafenib [18]. The interaction of these drugs with RET is described in Section 5.3. See Ref. [29] for a discussion of the treatment of the various types of small cell and non-small cell lung cancers.

4. Properties of the RET protein-tyrosine kinase domain

4.1. Primary, secondary, and tertiary structures of the human RET catalytic domain

The catalytic domain of RET consists of 310 amino acid residues; this is somewhat larger than the average domain of 275–300 residues owing to a kinase insert of 15 amino acid residues. The stoichiometry of the reaction catalyzed by RET protein-tyrosine kinase is given by the following chemical equation:

$$MgATP^{1-} + \text{protein-tyrosine–O : H} \rightarrow \text{protein-tyrosine–O : } PO_3{}^{2-} + MgADP + H^+$$

Note that the phosphoryl group ($PO_3{}^{2-}$) and not the phosphate ($OPO_3{}^{2-}$) group is transferred from ATP to the protein/peptide substrate.

Based on the sequences of five dozen protein-tyrosine and protein-serine/threonine kinases, Hanks and Hunter divided the primary structures of these enzymes into 12 domains (I-VIA, VIB-XI) [30]. Domain I of RET contains a glycine-rich loop (GRL) with a GxGxΦG signature (^{731}GEGEFG^{736}), where Φ refers to a hydrophobic residue and is phenylalanine in the case of RET. The glycine-rich loop occurs between the β1- and β2-strands and overlays the ATP/ADP-binding site (Fig. 3A). Because of its role in ATP binding and ADP release, the loop must be flexible and protein segments including glycine possess this property. In active RET proteins, the glycine-rich loop has an open configuration (PDB ID: 4CKJ) while in an inactive form, the glycine-rich loop has a closed configuration (PDB ID: 4CKI) (Fig. 3A). This distinction has not been reported in other protein kinases and it may be a unique feature of RET.

Domain II of RET contains a conserved Ala-Xxx-Lys (^{756}AVK^{758}) sequence in the β3-strand and domain III contains a conserved glutamate (E775) in the αC-helix that forms a salt bridge with a conserved β3-lysine (Fig. 3C) while in an active protein kinase conformation. Domain VIB of RET contains a conserved HRD sequence, which forms part of the catalytic loop (^{872}HRDLAARN^{879}). Domain VII contains an ^{892}DFG^{894} signature and domain VIII contains a ^{919}AIE^{921} sequence, which together represent the beginning and end of the RET activation segment. Note that most activation segments end with APE. The activation segment exhibits different conformations in active and dormant protein kinase states. Protein kinase domains IX–XI make up the αE–αI helices (Fig. 3A and B).

The original X-ray structure of the protein kinase A catalytic subunit provided an invaluable framework for understanding the interrelationship of the 12 domains and it has clarified our views on the fundamental biochemistry of the entire protein kinase superfamily (2CPK) [31,32]. All protein kinases including RET have a small amino-terminal and a large carboxyterminal lobe. The small lobe contains five conserved β-strands (β1–5) and an important regulatory αC-helix. The large lobe has four conserved short strands (β6–β9) along with seven helices (αD-αI and αEF) (Fig. 3A and B).

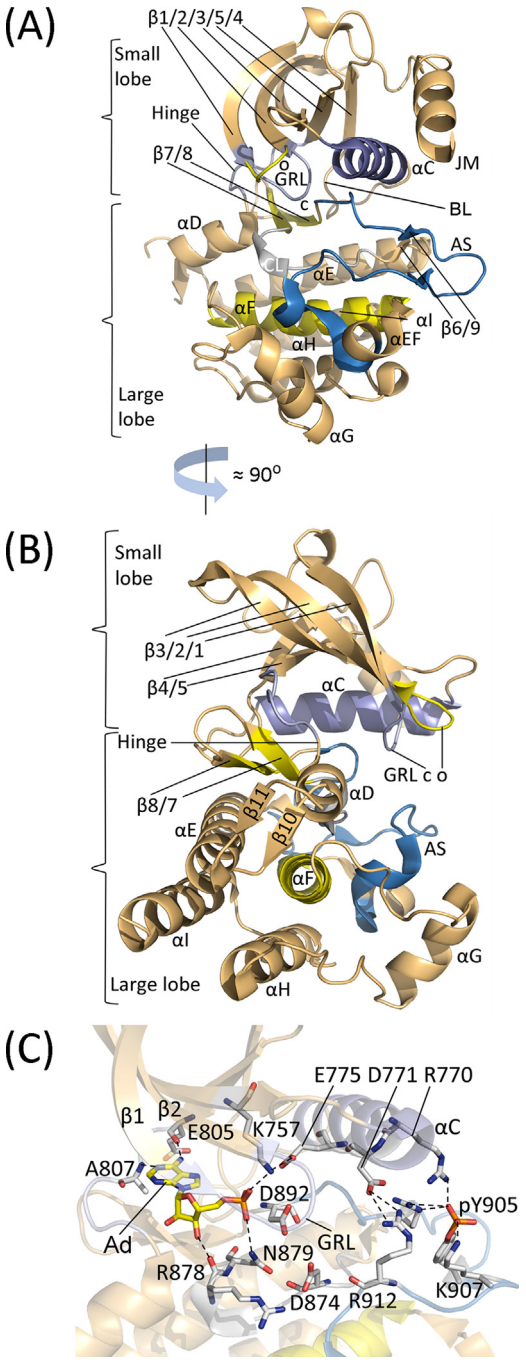

Fig. 3. Secondary and tertiary structure of the RET protein kinase domain. (A) Classical or frontal view of the protein kinase domain. (B) Side view. (C) AMP-binding site. The dashed lines depict polar bonds. Ad, adenine; AS, activation segment; BL, αC-β4 back loop; CL, catalytic loop; GRL, glycine-rich loop; JM, juxtamembrane segment; c, closed conformation of the GRL; o, open conformation of the GRL. (A) and (B) depict the superposition of the closed (PDB ID: 4CKI) and open (PDB ID: 4CKJ) glycine-rich loop structures of RET and (C) is derived from PDB ID: 2IVT. Figs. 3–5, 7, and 9 were prepared using the PyMOL Molecular Graphics System Version 1.5.0.4 Schrödinger, LLC.

All of the thousands of protein kinase structures that have been determined possess the canonical protein kinase structure as first described for the protein kinase A catalytic subunit [31–33].

A K/E/D/D (Lys/Glu/Asp/Asp) signature is found in all catalytically active protein kinases and these residues play a critical role during catalysis (Table 4) [33]. The lysine and glutamate are located in the small lobe and the two aspartate residues are located in the large lobe. Although ATP binds in a crevice between the two lobes, there is more extensive interaction with the amino-terminal lobe. An electrostatic bond linking the β3-lysine and the αC-glutamate is required for the formation of an active protein kinase, which corresponds to an αC_{in} configuration (Fig. 4A). These residues in many inactive enzyme conformations fail to make electrostatic contact and constitute an inactive αC_{out} structure (Fig. 4E) (See Refs. [33,34] for details). The αC_{in} structure is necessary, but not sufficient, for the expression of catalytic activity.

The large lobe participates in protein substrate binding and contains residues in the catalytic loop that play an essential role in the phosphoryl transfer reaction. Furthermore, two Mg^{2+} ions participate in the catalytic cycle of several protein kinases [35] and are most likely required for the functioning of RET. Of the X-ray structures of RET that are in the public domain, none contains ATP, a peptide substrate, or Mg^{2+}. By inference, however, RET D892 (the DFG-D and the first D of K/E/D/D) binds to $Mg^{2+}(1)$, which in turn binds to the β- and γ-phosphates of ATP. In this active conformation, the DFG-D is directed inward toward the active site. Moreover, RET N879 of the catalytic loop is hypothesized to bind $Mg^{2+}(2)$, which in turn binds to the α- and γ-phosphates of ATP. Both active and dormant protein kinases contain an additional helix (αEF) near the end of the activation segment (Fig. 3A).

Although no structure of RET with bound ATP/ADP is in the public domain, an activated and phosphorylated form of RET containing AMP has been described (PDB ID: 2IVT). This structure shows that the exocyclic 6-amino nitrogen of AMP forms a hydrogen bond with the carbonyl backbone residue of the first RET hinge residue (E805) that connects the small and large lobes of the protein kinase domain and the *N*1 nitrogen of the adenine base forms a second hydrogen bond with the N–H group of the third hinge residue (A807) (Fig. 3C). The adenine base of ATP/ADP is expected to bind in a similar fashion as described for many protein kinases [33]. As noted later, most small-molecule steady-state ATP competitive inhibitors of protein kinases including RET make one or more hydrogen bonds with backbone residues of the connecting hinge. The phosphate group of pY905 within the activation segment of RET forms a salt bridge with R897 and K907 also in the activation segment and R770 within the αC-helix. An additional electrostatic bond forms between R912 of the activation segment and D771 of the αC-helix (Fig. 3C). Although the activation segment pT197 of PKA interacts with H87 of the αC-helix (PDB ID: 1ATP), the interaction of protein-tyrosine kinase activation segment phosphotyrosine residues with the αC-helix as described here is uncommon.

The activation segment interacts with the protein substrate and consequently plays an important role in catalysis [36]. The proximal portion of the segment is located near the amino-terminus of the αC-helix and the catalytic loop HRD. The interfaces of these components are linked by hydrophobic interactions. Phosphorylation of a residue or residues within the activation segment converts a less-active to a more-active enzyme in most protein kinases [37], but this is not the case for RET. Although RET contain two phosphorylatable tyrosine residues (Y900, Y905) within the activation segment, Plaza-Menacho et al. reported that phosphorylation and activation of RET occurs following phosphorylation of Y697 within the juxtamembrane segment and of Y1062 within the C-terminal tail and phosphorylation of Y900 and Y905 occurs later [7,9]. Activation segment phosphorylation is also not required for the activation of the EGFR/ErbB1, ErbB3, and ErbB4 receptor protein-tyrosine kinases [38].

Plaza-Menacho reported that S909 within the activation loop also undergoes phosphorylation as catalyzed by RET [9]. This finding thus classifies RET as a dual specificity kinase, like MEK1/2 [39], that is able to mediate the phosphorylation of both tyrosine and serine residues. Plaza-Menacho also reported that the activation-loop pS909 interacts with the HRD motif and promotes both regulatory-spine assembly (described in Section 4.2) and

Table 4
Important human RET residues.[a]

	RET residues	Comments	Hanks no.
No. of residues	1114 (RET51)/1072 (RET9)		
Molecular Wt (kDa)[b]	124.3/119.8		
Signal sequence	1–28		
Extracellular domain	29–635	Ligand binding	
	CD1, 28–154[c]		
	CD2, 167–270[c]		
	CD3, 273–387[c]		
	CD4, 402–503[c]		
	Cys-rich 514–656	Receptor dimer formation	
Transmembrane segment	636–657	Links extracellular and intracellular domains and mediates dimer formation	
Juxtamembrane segment	658–723	Signal transduction	None
Juxtamembrane segment phosphorylation sites	Y687/S696	Binds PTPN11/RAC1 GTPase activation	None
Protein kinase domain	724–1016	Catalyzes substrate phosphorylation	
Glycine-rich loop	^{731}GEGEFG^{736}	Anchors ATP β- and γ-phosphates	I
β3-K of K/E/D/D	K757	Forms salt bridges with ATP α- and β-phosphates and with β3-K	II
αC-E, E of K/E/D/D	E775	Forms salt bridges with β3-K	III
Hinge residues	^{805}EYAKYG^{810}	Connects N- and C-lobes and hydrogen bonds with the ATP adenine	V
Kinase insert domain	826–840	Unclear	None
Kinase domain phosphorylation sites	(Y806, Y809)/Y1015	Unclear	(V)/None
Catalytic loop	^{872}HRDLAARN^{879}	Plays both structural and catalytic functions	VIb
Catalytic loop HRD-D, first D of K/E/D/D	D874	Catalytic base (abstracts protein substrate proton)	VIb
Catalytic loop HRDLAARN-N	N879	Chelates Mg^{2+}(2)	VIb
AS DFG-D, second D of K/E/D/D	D892	Chelates Mg^{2+}(1)	VII
AS	D892–E921	Enzyme activity/positions protein substrate	VII–VIII
AS phosphorylation sites	(Y900, Y905)/Y981	(Stabilizes the AS after phosphorylation)/unclear	VIII
End of AS	^{919}AIE^{921}	Interacts with the αHI loop and stabilizes the AS	VIII
C-terminal tail	1017–1114	Intracellular signaling	None
C-terminal tail phosphorylation sites	Y1062, Y1090, Y1096	Mediate intracellular signaling	None

[a] AS, activation segment; CD, cadherin-like segment; from UniProtKB ID: P07949.
[b] Molecular weight of the unprocessed and nonglycosylated precursor.
[c] From Ref. [13].

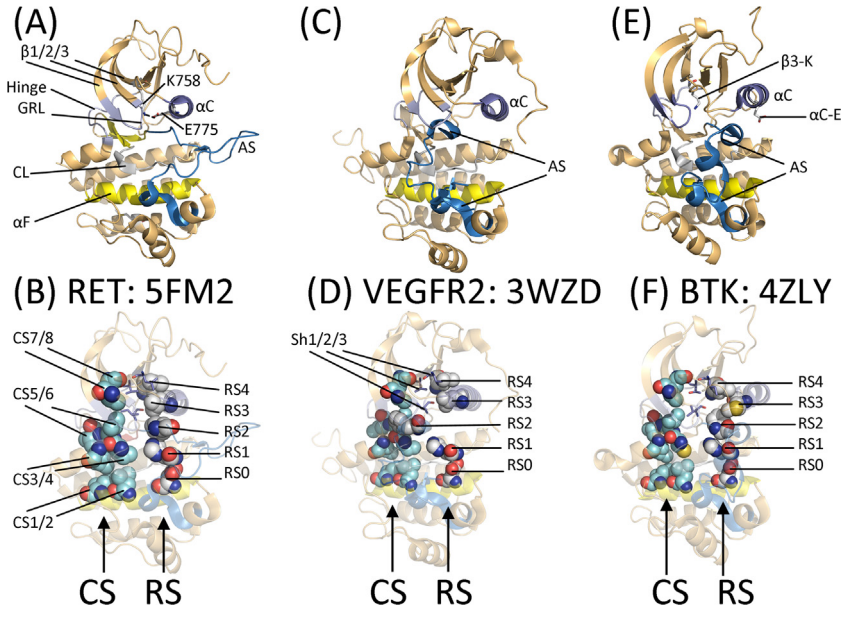

Fig. 4. Overview of the structures of (A) active RET, (B) the RET spines, (C) VEGFR2 with DFG-D_{out} (D) the VEGFR2 spines and shell residues, (E) BTK with αC_{out}, and (F) the BTK spines. Ad, adenine; AS, activation segment; CL, catalytic loop; CS, catalytic spine; GRL, glycine-rich loop; RS, regulatory spine; Sh, shell.

accessibility to phosphotyrosine binding modules [9]. Thus, pY905 is displaced and adopts a solvent-accessible conformation that is competent for a signaling function while apparently not playing an activating role.

Lemmon and Schlessinger reviewed the mechanisms of regulation of the receptor tyrosine-protein kinase family and most of these mechanisms involve ligand-induced receptor dimer formation and subsequent protein kinase activation, or they involve ligand-induced activation of pre-formed dimers [6]. During the activation process, one member of the dimer pair catalyzes the phosphorylation of activation segment tyrosine residues of the receptor partner (*trans* phosphorylation) along with the phosphorylation of other protein-tyrosines that create docking sites for signal transduction proteins that typically contain Src homology 2 (SH2) or phosphotyrosine-binding (PTB) domains [6]. Plaza-Menacho et al. demonstrated that the rate of RET phosphorylation was proportional to the enzyme concentration [7]. This confirms that phosphorylation is intermolecular and occurs in *trans*. If phos-

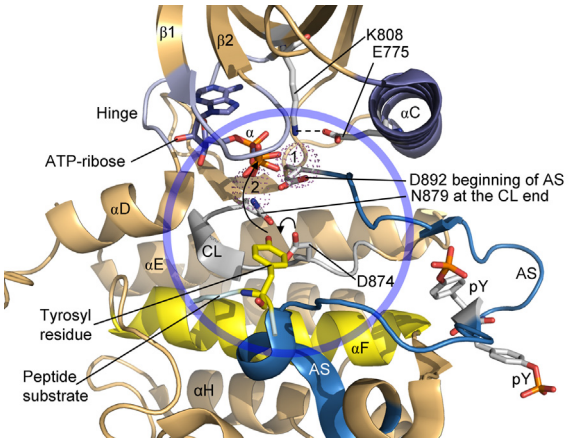

Fig. 5. Inferred mechanism of the RET catalyzed protein kinase reaction. D874 abstracts a proton from the tyrosyl substrate allowing for its nucleophilic attack onto the γ-phosphate of ATP. The chemistry occurs within the blue circle. 1 and 2 label the two Mg^{2+} ions. AS, activation segment; CL, catalytic loop. The figure was prepared from FGFR2 (PDB ID: 2PVF), but the numbers correspond to those of RET.

phorylation were intramolecular, the rate of RET phosphorylation would be independent of the enzyme concentration. RET dimerization is required for its activation except that activation segment phosphorylation is not required to increase catalytic activity. In the case of RET fusion proteins, the fusion partner is responsible for the dimerization that results in the subsequent activation of the protein kinase domain [17,18].

The RET catalytic loop within the large lobe consists of the canonical ^{872}HRDLAARN^{879} sequence. The catalytic aspartate (D874), which is the first D of K/E/D/D, abstracts a proton from the protein-tyrosine substrate residue thereby facilitating the in-line nucleophilic attack of the tyrosyl residue onto the γ-phosphorus atom of ATP (Fig. 5) [40]. Beside RET, the catalytic segment AAR sequence occurs in many receptor protein-tyrosine kinases including EGFR and PDGFRβ while RAA occurs in many non-receptor protein-tyrosine kinases such as Src [30].

4.2. The hydrophobic spines of human RET, VEGFR2, Bruton tyrosine kinase, and murine PKA catalytic domains

Kornev et al. investigated the tertiary structures of 23 protein kinases and they ascertained the role of several critical amino acid residues by a local spatial pattern alignment algorithm [41,42]. They classified four hydrophobic residues as a regulatory or R-spine [41] and eight hydrophobic residues as a catalytic or C-spine [42]. These spines contain amino acid residues from both the small and large lobes. The R-spine contains one residue from the regulatory αC-helix and another from the activation segment, both of which are major components that determine active or dormant enzyme states. The base of the R-spine within the large lobe anchors the catalytic loop and activation segment in an active state while the C-spine tethers the adenine base of ATP within the interlobe cleft thereby enabling catalysis. Moreover, the accurate alignment of both spines is necessary for the assembly of an active enzyme as described for ALK, Bruton tyrosine kinase, CDKs, ERK1/2, MEK1/2, the Janus kinases, Src, EGFR, ROS1, and VEGFR2 [29,35,43–50].

Going from the bottom to the top, the protein kinase regulatory spine consists of the catalytic loop HRD-H, the activation loop DFG-F, an amino acid four residues C-terminal to the conserved αC-glutamate, and an amino acid at the beginning of the β4-strand [41,42]. The backbone N–H of the HRD-H hydrogen bonds with an invariant aspartyl carboxyl group within the hydrophobic αF-helix. Going from the bottom to the top of the spine, Meharena et al. named the R-spine residues RS0, RS1, RS2, RS3, and RS4 (Fig. 4B) [51]. The R-spine of active RET is linear. The R-spine of dormant enzymes is usually nonlinear or broken, particularly involving the RS2 and RS3 residues. In the case of the DFG-D_{out} conformation, RS2 is displaced leftward (Fig. 4D) and in the case of the αC_{out} configuration, RS2 is displaced rightward (Fig. 4F).

The C-spine of protein kinases contains residues from both the small and large lobes. This spine is completed by the adenine base of ATP (Fig. 4B) [42]. The two residues of the amino-terminal lobe that interact with the adenine moiety of ATP include a conserved valine residue in the proximal portion of the β2-strand (CS7) and the canonical alanine from the AxK signature of the β3-strand (CS8). Moreover, a hydrophobic residue from the β7-strand (CS6) that is two residues carboxyterminal to the end of the catalytic loop interacts with the adenine portion of ATP. Nearly all steady-state ATP-competitive protein kinase inhibitors interact with CS6. The CS6 residue occurs between two hydrophobic residues (CS4 and CS5) that interact with the CS3 residue near the beginning of the αD-helix of the carboxyterminal lobe (Fig. 4B). CS5/6/4 immediately follow the catalytic loop asparagine (HRDxxxxN) so that one can readily identify these residues based upon the primary structure. Finally, CS3 and CS4 make hydrophobic contacts with the CS1 and CS2 residues of the αF-helix thereby forming a completed catalytic spine (Fig. 4B) [42]. Note that the hydrophobic αF-helix, which spans the entire large lobe, supports both spines. Furthermore, both spines play an indispensable role in anchoring the protein kinase catalytic residues in an active conformation. CS7 and CS8 in the small lobe make up the "ceiling" of the adenine-binding pocket while CS5/6/4 make up the "floor" of the binding pocket. Note that CS5/6/4 form the β7-strand (Fig. 3A) of the protein kinase domain.

Based upon the findings of site-directed mutagenesis studies, Meharena et al. identified three shell (Sh) residues in the protein kinase A catalytic subunit that support and stabilize the R-spine, which they labeled Sh1, Sh2, and Sh3 [51]. Sh2 corresponds to the so-called gatekeeper residue, which occurs just before the hinge. This term describes the role that the gatekeeper plays in controlling access to the back cleft or back pocket [52,53], which is also called hydrophobic pocket II (HPII) [53,54]. In contrast to the identification of the AxK, HRD, or DFG signatures, which is based upon their primary structures [30], the spines were identified by their spatial locations in active or dormant protein kinases [41,42]. Table 5 provides a summary of the spine and shell residues of RET, VEGFR2, BTK, and PKA. As described in Section 5.3, small molecule protein kinase antagonists often interact with residues that constitute the C-spine as well as the R-spine and the shell residues [58].

The RET X-ray structures are those of an active protein kinase (Fig. 4A and B). For example, the DFG-Asp is pointed inward toward the active site, the configuration of the αC-helix is in its active αC_{in} configuration with E775 forming a hydrogen bond with the β3-K808, and the catalytic and regulatory spines are linear and are neither bent nor broken. Moreover, the glycine-rich loop is in an open configuration that can readily accommodate ATP.

5. Drugs approved and in clinical trials for the treatment of RET-driven thyroid and lung cancers

5.1. Clinical trial summary

Currently the FDA has approved (i) cabozantinib and vandetanib for the treatment of medullary thyroid cancers and (ii) lenvatinib and sorafenib for differentiated thyroid cancers (Table 6). In addition, these and other drugs are in clinical trials for the treatment of both thyroid and RET-driven lung cancers. It should be noted that using the code for the RET inhibitors is useful for literature searches in both PubMed and PDB data bases because it often results in list-

Table 5
Spine and shell residues of human RET, VEGFR2, BTK, and murine PKA.

	Symbol	KLIFS No.[a]	RET	VEGFR2	BTK	PKA[b]
Regulatory spine						
β4-strand (N-lobe)	RS4	38	L790	L901	L460	L106
C-helix (N-lobe)	RS3	28	L779	L889	M449	L95
Activation loop F of DFG (C-lobe)	RS2	82	F893	F1047	F540	F185
Catalytic loop His/Tyr (C-lobe)	RS1	68	H872	H1026	H519	Y164
F-helix (C-lobe)	RS0	None	D933	D1087	D579	D220
R-shell						
Two residues upstream from the gatekeeper	Sh3	43	L802	V914	I472	M118
Gatekeeper, end of β5-strand	Sh2	45	V804	V916	T474	M120
αC-β4 back loop	Sh1	36	I788	V899	V458	V104
Catalytic spine						
β3-AxK motif (N-lobe)	CS8	15	A756	A866	A428	A70
β2-strand (N-lobe)	CS7	11	V738	V848	V416	V57
β7-strand (C-lobe)	CS6	77	L881	L1035	L528	L173
β7-strand (C-lobe)	CS5	78	V822	L1036	V529	I174
β7-strand (C-lobe)	CS4	76	I880	I1034	C527	L172
D-helix (C-lobe)	CS3	53	L812	L924	L482	M128
F-helix (C-lobe)	CS2	None	L940	L1094	L586	L227
F-helix (C-lobe)	CS1	None	I944	I1098	I590	M231

[a] KLIFS (kinase–ligand interaction fingerprint and structure) from Ref. [55].
[b] From Refs. [41,42,51].

Table 6
Properties of selected orally effective small molecule RET multikinase inhibitors.

Name, code, trade name®	Selected targets	PubChem CID[a]	Formula	MW (Da)	D/A[b]	RET IC_{50} (nM)	FDA-approved indications (year)[c]
Alectinib, CH 5424802, Alcensa®	RET, ALK	49806720	$C_{30}H_{34}N_4O_2$	482.6	1/5	4.8[d]	ALK^+ NSCLC (2015)
Cabozantinib, XL-184 and BMS-907351, Cometriq®	RET, VEGFR1/2/3, MET, Kit, Flt-3, Tie-2, TrkB, Axl, ROS1	25102847	$C_{28}H_{24}FN_3O_5$	501.5	2/7	5–10[e]	Medullary thyroid cancer (2012); RCC (2016) after one prior anti-angiogenic therapy
Lenvatinib, E7080, Lenvima®	RET, VEGFR2, FGFR1/2/3/4, PDGFRα, Kit	9823820	$C_{21}H_{19}ClN_4O_4$	426.9	3/5	1.5[e]	Differentiated thyroid cancer refractory to radioiodine treatment (2015); RCC (2016) in combination with everolimus after one anti-angiogenic therapy
Ponatinib, AP24534, Iclusig®	RET, VEGFR1/2/3, PDGFRα/β, FGFR1/2/3/4, BCR-Abl, Kit, Tie2, Fl33, EphR, Src family kinases	24826799	$C_{29}H_{27}F_3N_6O$	532.6	1/8	26[e]	CML (2012), Ph^+ ALL (2012)
Sorafenib, BAY 43–9006, Nexavar®	RET, Raf, Kit, Flt3, VEGFR1/2/3, PDGFRβ	216239	$C_{21}H_{16}ClF_3N_4O_3$	464.8	3/7	6–47[e]	RCC (2005); HCC (2007); Differentiated thyroid cancer refractory to radioiodine treatment (2013)
Sunitinib, SU-11248, Sutent®	RET, PDGFRα/β, VEGFR1/2/3, Kit, CSF-1R, Flt3	5329102	$C_{22}H_{27}FN_4O_2$	398.4	3/4	220[e]	RCC (2006), GIST (2006), pNET (2011)
Vandetanib, ZD6474, Caprelsa®	RET, EGFRs, VEGFRs, Brk, Tie2, EphRs, Src family kinases	3081361	$C_{22}H_{24}BrFN_4O_2$	475.3	1/7	100[e]	Medullary thyroid cancer (2011)

[a] www.ncbi.nlm.nih.gov/pccompound.
[b] No. of hydrogen bond donors/acceptors.
[c] ALL, acute lymphoblastic leukemia; CML, chronic myelogenous leukemia; GIST, gastrointestinal stromal tumor; HCC, hepatocellular carcinoma; NSCLC, non-small cell lung cancer; Ph^+, Philadelphia chromosome positive; pNET, pancreatic neuroendocrine tumor; RCC, renal cell carcinoma.
[d] Ref. [56].
[e] Ref. [57].

ings that are missed when using the generic or trade names. See Ref. [18,24,59–61] for a summary of the clinical trials that led to the approval of the four drugs for the treatment of thyroid cancers and for the status of the other drugs that are in clinical trials for the treatment of thyroid and RET-driven lung cancers.

5.2. Classification of protein kinase-drug complexes

Dar and Shokat identified three categories of small molecule protein kinase inhibitors: types I, II, and III [62]. Type I inhibitors bind within the ATP pocket of an active conformation of the kinase domain; type II inhibitors bind to an inactive (usually DFG-D_{out}) conformation of the enzyme while type III inhibitors bind at an allosteric site. Allosteric inhibitors bind to a location that is distinct from the active site [63] or outside of the ATP-binding pocket. Zuccotto defined type I½ inhibitors as ligands that bind to inactive protein kinases with the DFG-Asp directed inward toward the active site (in contrast to the DFG-D_{out} structure) [64]. The inactive enzyme may have the αC_{out} conformation or it may exhibit abnormalities in the regulatory spine or the activation

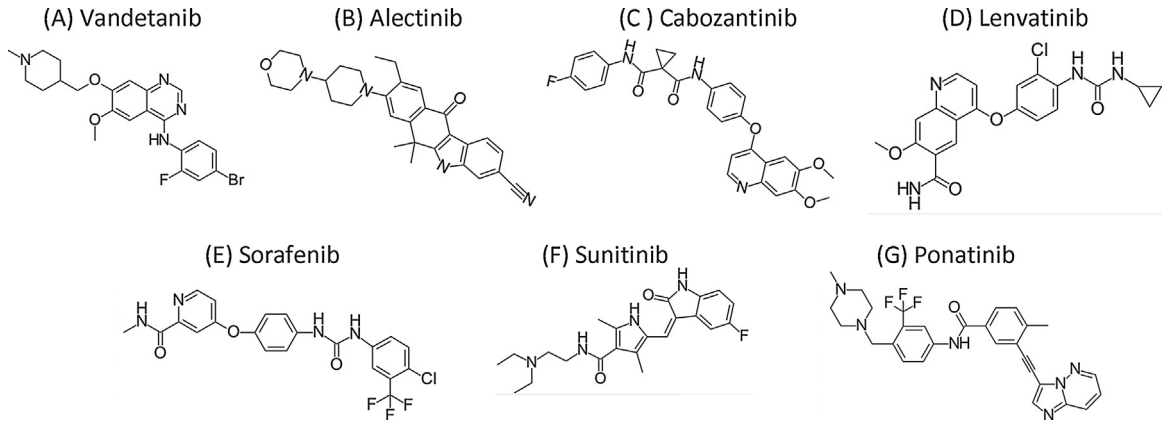

Fig. 6. Structures of selected RET multikinase inhibitors.

segment. Subsequently, Gavrin and Saiah divided allosteric antagonists into two classes: III and IV [65]. Thus, type III inhibitors bind within the crevice between the small and large lobes contiguous with, but independent of, the ATP binding pocket while type IV allosteric inhibitors bind elsewhere. Lamba and Gosh defined bivalent inhibitors as those antagonists which span two separate sections of the protein kinase domain as type V inhibitors [66]. An antagonist that binds to both the ATP-binding site and the peptide substrate side would be classified as a type V inhibitor. To complete this classification, we labeled small molecules that form covalent adducts with the target enzyme as type VI inhibitors [58]. Afatinib is a type VI inhibitor of EGFR that is FDA-approved for the treatment of NSCLC (www.brimr.org/PKI/PKIs.htm). However, this drug binds initially to an active conformation of EGFR (like a type I inhibitor) and then the thiol group of C797 forms a covalent adduct with the drug [58].

We have previously classified the type I½ and type II inhibitors into A and B subtypes [58]. Sorafenib is a type II inhibitor of VEGFR2 (PDB ID: 4ASD). This drug binds to this protein with the DFG-D_{out} configuration and extends into the back cleft [58] and we classified drugs that extend into the back cleft as type A inhibitors. In contrast, we classified drugs such as sunitinib that bind to the DFG-D_{out} conformation of VEGFR2 while not extending into the back cleft as type B inhibitors (PDB ID: 4AGD). Based on limited data [58], the practical consequence of this distinction is that type A antagonists bind to their target kinase with a long residence time when compared with type B inhibitors. In the next section, we will see that the RET antagonists studied in this paper are type I inhibitors.

5.3. Structures of RET-drug complexes

The following provides an overview of drug-RET protein kinase catalytic domain interactions. Several RET steady-state ATP-competitive inhibitors bind to CS7 and CS8 within the small lobe and CS6 within the large lobe. These residues form hydrophobic contacts with the adenine base of ATP. Although protein kinase antagonists may form 1–3 hydrogen bonds with the backbone residues within the hinge, the RET inhibitors form a single hydrogen bond with the N—H group of A807 within the hinge. Many drugs interact with the gatekeeper residue by forming hydrogen bonds or by making hydrophobic contact with the −R group. Because the RET gatekeeper is valine, interaction with the gatekeeper is expected to be hydrophobic in nature and several RET antagonists interact with this residue. Moreover, several RET antagonists interact with residues within the αC-β4 back loop, particularly the Sh1 residue. Many protein kinase antagonists bind to residues within the back pocket that extends past the gatekeeper toward the activation segment and the αC-helix. All of the RET inhibitors interact with residues within the selectivity entrance near the solvent front including those at the end of the β1-strand just before the G-rich loop in the amino-terminal lobe and those in the αD-helix within the carboxyterminal lobe; these residues form the mouth of the front pocket. The so-called selectivity pocket includes residues near the αC-helix and β5-strand within the back pocket, residues near the β3-lysine, the αC-glutamate, and DFG-D, but it excludes residues that contact the adenine base of ATP including CS6/7/8 [67].

Vandetinib (*N*-(4-bromo-2-fluorophenyl)-6-methoxy-7-((1-methylpiperidin-4-yl) methoxy) quinazolin-4-amine) (Fig. 6A) is a multikinase inhibitor that was approved by the FDA for the treatment of medullary thyroid cancer in 2011 (www.brimr.org/PKI/PKIs.htm). Knowles et al. determined the X-ray crystal structure of vandetanib bound to RET [11]. Most targeted protein kinase antagonists form hydrogen bonds with amino acid residues within the hinge and vandetanib is not an exception. They found that *N*1 of the quinazoline group forms a hydrogen bond with the N—H group of A807 within the hinge (Fig. 7A). They also found that the drug made hydrophobic contact with L730 at the end of the β1-strand, V738 at the beginning of the β2-strand, A756 (CS8), V757 and K758 within the β3-strand, L779 (RS3) within the αC-helix, L801 near the beginning of the β5-strand, I803 and the V804 gatekeeper at the end of the β5-strand, Y806 within the hinge, and L881 (CS6) within the β7-strand on the floor of the adenine pocket.

Liao [54] and van Linden et al. [55] divided the region between the small and large lobes into a front cleft or pocket, a gate area, and a back cleft (Fig. 8). Hydrophobic pocket II (HPII) or the back pocket consists of the gate region and the back cleft. The front pocket includes the Gly-rich loop, the hinge, the segment connecting the hinge to the αD-helix in the carboxyterminal lobe, and amino acid residues within the catalytic loop. The gate region includes amino acids within the β3-strand and the proximal portion of the activation segment including DFG. These investigators also depicted several sub-pockets within these three fields. Accordingly, the front cleft contains an adenine pocket (AP) adjacent to two front pockets (FP-I and FP-II) and the gate region contains two back pockets (BP-I-A and BP-I-B). The back cleft borders the αC-helix, the αC-β4 loop, part of the β4 and β5-strands, and part of the αE-helix. The X-ray structure shows that vandetanib binds to the RET front pocket and gate region including BP-I-A and BP-I-B (http://klifs.vu-compmedchem.nl/; PDB ID: 2IVU). The methylpiperidine group extends away from the RET protein kinase domain into the solvent. The X-ray crystallographic structure shows that RET is in an active conformation with an open glycine-rich loop, αC-E775 forming a hydrogen bond with the β3-K758, a linear R-spine with DFG-D892 pointing inward toward the active site, and an activation segment

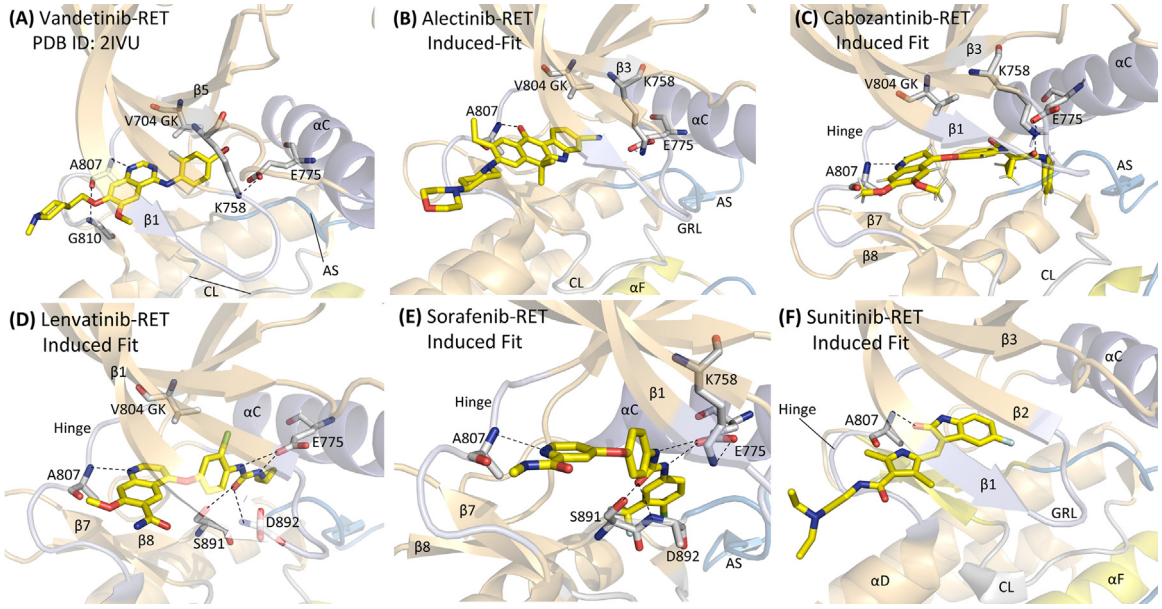

Fig. 7. Structures of RET-drug complexes. The dashed lines depict polar bonds.

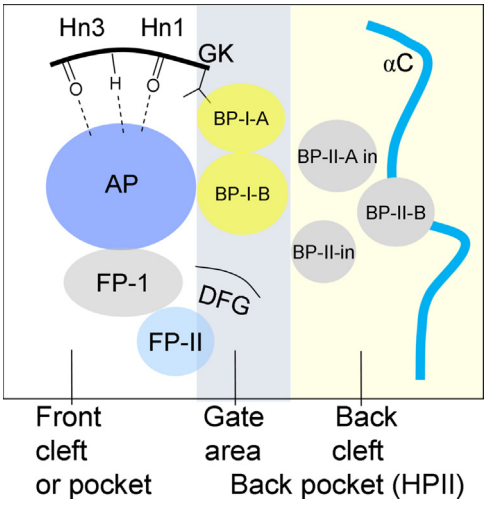

Fig. 8. Structure of the protein kinase domain drug binding pocket. AP, adenine pocket; BP, back pocket; FP, front pocket; Hn, hinge; HP, Hydrophobic pocket II. Adapted from Refs. [54,55].

in its open conformation. These structural studies indicate that vandetanib binds to an active conformation of RET and is thereby classified as a type I inhibitor [58].

van Linden et al. have created an all-inclusive summary of drug and ligand binding to more than 1200 human and mouse protein kinase catalytic domains [55]. Their KLIFS (kinase–ligand interaction fingerprint and structure) catalog includes the alignment of 85 protein kinase-ligand binding-site residues, which allows for the classification of ligands based upon their binding properties and facilitates the identification of related interaction features. These investigators established a standard residue numbering system that enables a comparison among all protein kinases. See Table 5 for the correspondence between the C-spine, Shell, and R-spine amino acid residues and those of the KLIFS database. Furthermore, these investigators established a valuable searchable and noncommercial web site that is continuously updated and provides information on protein kinase-ligand interactions (http://www.vu-compmedchem.nl/).

Alectinib (9-ethyl-6,6-dimethyl-8-(4-morpholin-4-ylpiperidin-1-yl)-11-oxo-5H-benzo[*b*]carbazole-3-carbohitrile) (Fig. 6B) is an ALK/RET antagonist that is approved for the treatment of ALK$^+$ NSCLC. No X-ray structural studies of alectinib bound to RET have been reported. To obtain an idea on the possible interaction of this drug with the enzyme, the Schrödinger Induced Fit Docking Protocol (2016-1 release) was used to dock the drug into phosphorylated human RET (with the initially bound pyrazolo[3,4-*d*] pyrimidine called PP-1, PDB ID: 5FM2) [68]. The induced-fit pose indicates that the 11-oxo group of the drug forms a hydrogen bond with the N—H group of RET A807 of the hinge (Fig. 7B). Alectinib makes hydrophobic contacts with L730 at the end of the β1-strand, the β3-A756 (CS8), I788 (Sh1) of the αC-β4 back loop, the V804 gatekeeper at the end of the β5-strand, Y806 within the hinge, L881 (CS6) within the β7-strand of the large lobe. The drug makes van der Waals contact with S891, the residue immediately before DFG-D892 of the activation segment. L730 and A756 occur above the plane of the scaffold while L881 occurs below the plane. These residues are found within the front pocket and BP-I-B in the gate area. The 4-morpholin-4-piperidine group extends from the enzyme into the solvent. The glycine-rich loop is in an open configuration, αC-E775 forms a hydrogen bond with the β3-K758, the R-spine is linear, and DFG-D892 is pointed inward toward the active site, properties associated with an active enzyme form. These modeling studies indicate that alectinib is a type I inhibitor of RET owing to its interaction with a fully active enzyme [58].

Alectinib is a second-line treatment that is FDA-approved against crizotinib-resistant ALK$^+$ NSCLC (www.brimr.org/PKI/PKIs.htm). The binding of alectinib to ALK is similar to its binding to RET; however, the proximal portion of the activation segment of ALK forms an AL-helix and is autoinhibited and inactive thereby making it a type I½B ALK inhibitor where I½ refers to an inactive conformation with DFG-D_{in} and B indicates that the drug does not extend into the back cleft [29]. Alectinib binds to the front pocket and the BP-I-B subpocket of ALK (http://www.vu-compmedchem.nl/; PDB ID: 3AOX).

Cabozantinib (1-*N*-[4-(6,7-dimethoxyquinolin-4-yl) oxyphenyl]-1-*N*′-(4-fluorophenyl) cyclopropane-1,1-dicarboxamide) is a multikinase inhibitor that is FDA approved for the treatment of medullary thyroid cancer and renal cell carcinoma (Table 6). Although there are no structural data of cabozantinib

(Fig. 6C) binding to RET or any other protein kinase in the public domain, we were able to generate a satisfactory pose of the drug binding to human RET using the Schrödinger Induced Fit Docking Protocol as described above using PDB ID: 5FM2 as a template [68]. The resulting pose indicates that the cabozantinib quinoline *N*1 forms a hydrogen bond with the N—H group of A807 of the hinge and the distal carbonyl group forms a hydrogen bond with β3-K758 (Fig. 7C). The drug makes hydrophobic interactions with L730 at the end of the β1-strand, F735 within the G-rich loop, V738 (CS7) within the β2-strand, S774, V778, and L779 (RS3) within the αC-helix, I788 (Sh1) of the back loop, Y806 within the hinge, L870 (two residues before the catalytic loop), H872 within the catalytic loop (RS1), L881 (CS6) within the β7-strand, I890 at the end of the β8-strand, and DFG-F893 within the activation segment. The drug binds to an active conformation of RET and is thereby classified as a type I inhibitor [58].

Lenvatinib (4-[3-chloro-4-(cyclopropylcarbamoylamino) phenoxy]-7-methoxyquinoline-6-carboxamide) (Fig. 6D) is a multikinase inhibitor that was FDA-approved for the treatment of thyroid cancer in 2015 (Table 6). We generated a satisfactory pose of its binding to RET using the Schrödinger Induced Fit Docking program as described above using PDB ID: 5FM2 as a template [68]. We found that the *N*1 of the quinoline fragment forms a hydrogen bond with the N—H group of A807 of the hinge, the N—H groups of the urea moiety of the drug form hydrogen bonds with the carboxyl group of αC-E775, and the OH group of S891 and the N—H group of DFG-D892 forms a hydrogen bond with the lenvatinib urea oxygen (Fig. 7D). The drug makes hydrophobic contact with L730 at the end of the β1-strand, V738 (CS7) within the β2-strand, V778 and L779 (RS3) within the αC-helix, the V804 gatekeeper at the end of the β5-strand, L881 (CS6) within the β7-strand, and DFG-F893 within the activation segment. The drug binds to an active conformation of RET and is thereby classified as a type I inhibitor [58].

The binding of lenvatinib to VEGFR2 has been described (3WZD); the drug binds to the front pocket, gate area, and back pockets and the BP-I-B and BP-II-in subpockets (http://www.vu-compmedchem.nl/). DFG-D is pointed inward and the αC-helix is in its active conformation; however, the R-spine is in an inactive broken conformation so that the drug is classified as a type I½A inhibitor of VEGFR2 where I½ indicates an inactive conformation with DFG-D_{in} and A indicates that the drug extends into the back pocket [58]. That a given antagonist can bind to different conformations of its targets adds to the complexity of inhibitor classification. For example, bosutinib is a type I inhibitor of Src and a type IIB inhibitor of Abl, both of which are non-receptor protein-tyrosine kinases [58]. Crizotinib is a type I inhibitor of ALK but a type I½ B inhibitor of c-Met (hepatocyte growth factor receptor protein-tyrosine kinase), both of which are receptor protein-tyrosine kinases. Erlotinib is a type I and I½B inhibitor of EGFR. Moreover, sunitinib is a type I½B inhibitor of CDK2 (a protein-serine/threonine kinase) but a type IIB inhibitor of Kit (a receptor protein-tyrosine kinase). These findings reveal that protein kinase antagonists are not necessarily conformationally selective.

Sorafenib (4-[4-[[4-chloro-3-(trifluoromethyl)phenyl]carbamoy lamino]phenoxy]-N-methylpyridine-2-carboxamide) (Fig. 6E), a multikinase inhibitor, is FDA-approved for the treatment of differentiated thyroid cancer, hepatocellular carcinoma, and renal cell carcinoma (Table 6). We generated a satisfactory pose of its binding to RET using the Schrödinger Induced Fit Docking program as described above using 5FM2 as a template [68]; we found that the *N*1 of pyridine forms a hydrogen bond with the N—H group of A807 of the hinge, the urea N—H groups form hydrogen bonds with the carboxyl group of E775 of the αC-helix, and the urea oxygen forms a hydrogen bond with the —OH group of S891 and the N—H group of DFG-D892 (Fig. 7E). We found that the drug makes hydrophobic contact with L730 at the end of the β1-strand, V738 (CS7) within the β2-strand, V778 and L779 (RS3) of the αC-helix, V787 and I788 (Sh1) within the back loop, the V804 gatekeeper (Sh2) at the end of the β5-strand, HRD-H872 (R1), L881 (CS6) within the β7-strand, I890 (two residues before the activation segment), DFG-F893, and S896 within the activation segment.

Sorafenib is a type IIA inhibitor of B-Raf (PDB ID: 1UWH) and CDK8 (PDB ID: 3RGF) (both are nonreceptor protein-serine/threonine kinases); the II designation indicates that the DFG-D is directed away from the active site (DFG-D_{out}). In contrast, the induced-fit model has the drug binding to an active conformation of RET and is thereby classified as a type I inhibitor with DFG-D_{in} [58]. Gao et al. studied the interaction of sorafenib with RET with the DFG_{out} configuration using molecular modeling and molecular dynamics simulations with VEGFR2 as a template (PDB ID: 4ASD) [69]. They reported that the drug forms two hydrogen bonds with A807 in contrast to the one hydrogen bond that we found. Moreover, they found that the urea group of sorafenib formed two hydrogen bonds with RET involving E775 and D872, which is in agreement with our results. However, we found that the urea oxygen also forms a hydrogen bond with the —OH group of S891. The differences in the results of these two studies likely involves our selection of a RET template with the DFG-D_{in} vs. their selection of a template with the DFG-D_{out} configuration. As noted above, bosutinib and sunitinib have been shown to bind to both DFG-D_{in} and DFG-D_{out} configurations [58].

Sunitinib (*N*-[2-(diethylamino) ethyl]-5-[(Z)-(5-fluoro-2-oxo-1H-indol-3-ylidene) methyl]-2,4-dimethyl-1H-pyrrole-3-carboxamide) (Fig. 6F) is a multikinase inhibitor that is FDA-approved for the treatment of renal cell carcinoma, gastrointestinal stromal tumors, and pancreatic neuroendocrine tumors (Table 6). We generated a satisfactory pose of its binding to RET using the Schrödinger Induced Fit Docking program as described above using 5FM2 as a template [68]; the oxygen atom of the indolinone scaffold forms a hydrogen bond with the N—H group of A807 within the hinge (Fig. 7F). We found that the drug makes hydrophobic contacts with L730 at the end of the β1-strand, A756 (CS8), I788 (Sh1), the gatekeeper V804 residue, Y809 within the hinge, L881 (CS6), and DFG-D892. Because the RET protein kinase domain has all of the characteristics of an active enzyme, sunitinib is classified as a type I inhibitor of this enzyme. Sunitinib is a type I½B inhibitor of CDK2 and a type IIB inhibitor of Kit and VEGFR2 receptor protein-tyrosine kinases [58].

Ponatinib (3-(2-imidazo[1,2-*b*] pyridazin-3-ylethynyl)-4-methyl-N-[4-[(4-methylpiperazin-1-yl) methyl]-3-(trifluoromethyl) phenyl] benzamide) (Fig. 6G), a multikinase inhibitor, is approved for the treatment of chronic myelogenous and acute lymphoblastic leukemias (Table 6). Although the X-ray structures of ponatinib bound to FGFR1 (PDB ID: 4V04), FGFR4 (PDB ID: 4UXQ), Kit (PDB ID: 4U0I), and Abl (PDB ID: 3OXG) show that it is a type IIA inhibitor, there are no structures with the drug bound to RET. Unfortunately, we were unable to generate a satisfactory pose of its binding to RET using either of the Schrödinger Induced Fit or Glide programs [68,70]. It is possible that the Schrödinger programs were unable to model ponatinib docking into a type IIA RET ligand-binding site starting with a type I template.

To summarize this section, each of the drugs forms a hydrogen bond with the N—H group of A807, which is the third residue within the RET hinge. Each of the drugs also makes hydrophobic contacts with L730 at the end of the β1-strand before the G-rich loop and L881 (CS6) within the β7-strand on the floor of the active site. Except for cabozantinib, each drug makes hydrophobic contact with the V804 gatekeeper at the end of the β5-strand. Moreover, each drug makes hydrophobic contact with V738 (CS7) within the β2-strand with the exception of alectinib. Vandetanib,

alectinib, lenvatinib, and sunitinib make hydrophobic contact with A757 (CS8) within the β3-strand while vandetanib, alectinib, and cabozantinib make hydrophobic contact with Y806 within the hinge. Cabozantinib, lenvatinib, and sorafenib make hydrophobic contact with L779 (RS3) of the αC-helix. Cabozantinib and sorafenib interact with H872 (RS1) and I890 at the end of the β8-strand and lenvatinib and sorafenib make hydrophobic contact with DFG-F893 (RS2). Each of the drugs also makes contact with a number of other variable residues. The description of the C-spine (CS6/7/8), R-spine (RS1/2/3), and the shell residues (SH1/2/3) has served as a bellwether for interaction partners of targeted small molecule protein kinase antagonists.

The US FDA has approved 36 small molecule drugs that bind directly to the intracellular protein kinase domain (www.brimr.org/PKI/PKIs.htm). Table 7 provides an updated classification of FDA-approved protein kinase inhibitors based upon the structure of the drug-enzyme complexes as we have previously reported [29,58]. Of the 36 approved drugs, we are lacking X-ray crystal structures of acalabrutinib, cabozantinib, midostaurin, ibrutinib, osimertinib, pazopanib, regorafenib, trametinib bound to their drug targets and their consequent structure-based inhibitor classification. However, we do have computer-based models of cabozantinib, ibrutinib, and trametinib binding to target enzymes. The results indicate that 26 drug-enzyme complexes exhibit the DFG-D_{in} configuration (types I, I½A, I½B) and 13 complexes exhibit the DFG-D_{out} configuration (type IIA and IIB). There are two type III allosteric inhibitors that bind adjacent to the adenine pocket and two type VI irreversible, or covalent, inhibitors. We have no examples of FDA-approved type IV allosteric inhibitors, which do not bind adjacent to the adenine pocket, nor do we have any examples of approved type V bivalent inhibitors. Perhaps such inhibitors will be forthcoming in the future.

6. RET point mutations

Activating *RET* mutations within the extracellular cysteine-rich domain have been identified in patients with MEN2A and familial medullary thyroid cancer (FMTC) [24]. As a result of the conversion of cysteine to another amino acid residue, disruption of intramolecular disulfide bridges occurs thereby enabling the formation of intermolecular covalent disulfide bonds that lead to ligand-independent dimerization and activation. Three of the mutations are of non-cysteine residues (G533C, D631Y, and K666E) and it is unclear how these changes lead to activation of protein kinase activity. Activating *RET* mutations within the protein kinase domain have been identified in patients with MEN2B and occasionally in familial medullary carcinomas. These mutations are listed in Table 8.

The locations of the RET protein kinase domain mutations are depicted in Fig. 9. The clinically more serious mutations involve codons 883, 918, or V804M/E805K, V804M/Y806C, and V804M/S904C double mutations. Patients with these mutations should have a prophylactic thyroidectomy during the first year of life [15]. The codon 883 mutation (A883F) occurs at the end of the β7-strand within the catalytic loop and this mutation may enhance catalytic activity. The *RET* M918T mutation is associated with the most severe disease phenotypes and is the most transforming of all RET mutants in cultured cells [1]. This mutation occurs at the end of the activation segment near the protein-substrate binding site and this mutation may alter substrate affinity. Gujral et al. found that the M918T mutant was more highly phosphorylated in cell culture in response to GDNF stimulation when compared with the wild type protein [71]. Moreover, they reported that the mutation decreases autoinhibition by the activation segment. They also found that the mutation decreased the K_m for ATP from 188 to 105 μM while the

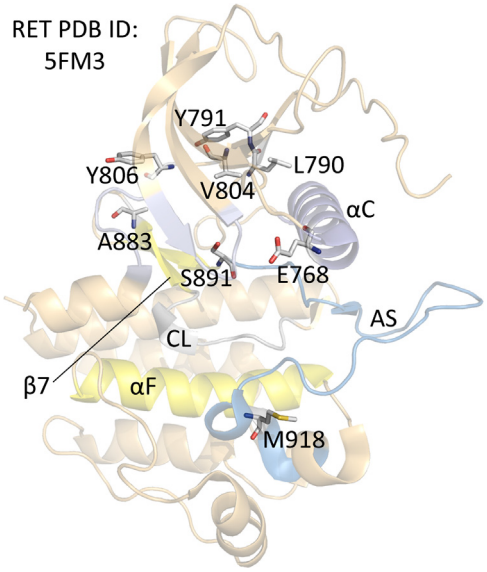

Fig. 9. Location of activating *RET* protein-tyrosine kinase point mutations.

K_d was decreased from 192 to 15.3 μM. Here we have a case where a mutation about 20 Å from the ATP-binding site is able to influence nucleotide binding. Furthermore, these investigators found evidence that the M918T mutant forms dimers more readily than the wild type protein. Thus, Gujral et al. concluded that multiple distinct, but complementary, mechanisms are responsible for the activation of the M918T mutant.

Each of the double mutations (V804M/E805K, V804M/Y806C, and V804M/S904C) involve the gatekeeper (V804), hinge residues (E805, Y806), or activation segment (S904) and such mutations may promote ATP binding. The less serious mutations involve codons 768, 790, 791, 804, and 891. Surgery on patients with these mutations can be delayed provided that they are carefully monitored [15]. The codon E768D mutation occurs near the beginning of the αC-helix. The carboxyl group of E768 forms a hydrogen bond with the S765 N—H group at the beginning of the αC-helix, but D768 is unable to form this bond. Moreover, E768 forms a salt bridge with K761, but D768 is unable to form this bond. These two electrostatic bonds in the wild type enzyme (E768) may produce a dormant enzyme conformation while their absence (D768) may promote an active state. The codon L790F or Y791F mutation occurs at the beginning of the β4-strand. L790 forms part of the regulatory spine and perhaps the mutation to phenylalanine strengthens the spine. The mutation of the adjacent Y791F may also affect the strength of the R-spine. The S891A is located just proximal to the activation segment and the —OH group of S891 forms a salt bridge with DFG-D892. An alanine at this position cannot form such an electrostatic bond and this may lead to activation of RET catalytic activity. From a mechanistic point of view, additional biochemical studies on the ability of these mutations to alter enzyme activity seem warranted.

7. Clinical outcomes in response to RET inhibitors

The clinical outcomes in response to RET-directed therapies are limited when compared with those achieved with other targeted therapies directed at other oncogenic drivers of solid tumors including EGFR, B-Raf, ALK, and ROS1 [24]. Cabozantinib and vandetanib are approved for the treatment of medullary thyroid cancer and lenvatinib and sorafenib are approved for the treatment of differentiated thyroid cancers (papillary and follicular). It is noteworthy that these have been approved regardless of the *RET* mutation status. Alectinib, ponatinib, and sunitinib are RET and

Table 7
Drug-protein kinase interactions.

Drug-enzyme[a]	PDB ID	DFG-D	AS[b]	αC	R-Spine	GK[c]	Inhibitor class	Pockets and sub-pockets occupied[d]
Alectinib-RET	Model	in	open	in	active	V	I	F, BP-I-B[e]
Bosutinib-Src	4MXO	in	open	in	active	T	I	F, G, BP-I-A/B
Cabozantinib-RET	Model	in	open	in	active	V	I	F, G, B, BP-I-B, BP-II-in, BP-II-B[e]
Dasatinib-Abl	2GQG	in	open	in	active	T	I	F, FP-I
Erlotinib-EGFR	1M17	in	open	in	active	T	I	F, G, BP-I-A/B
Gefitinib-EGFR	2ITY	in	open	in	active	T	I	F, G, BP-I-A/B
Lenvatinib-RET	Model	in	open	in	active	V	I	F, G, B, BP-I-B, BP-II-in[e]
Palbociclib-CDK6	2EUF	in	open	in	active	F	I	F
Ruxolitinib-Src[f]	4U5J	in	open	in	active	T	I	F[e]
Sorafenib-RET	Model	in	open	in	active	V	I	F, G, B, BP-I-B, BP-II-in[e]
Sunitinib-RET	Model	in	open	in	active	V	I	F, BP-I-B[e]
Tofacitinib-JAK3	3LXK	in	open	in	active	M	I	F, FP-I/II
Tofacitinib-JAK1	3EYG	in	open	in	active	M	I	F, FP-I/II
Vandetanib-RET	2IVU	in	open	in	active	V	I	F, G, BP-I-A/B
Dabrafenib-B-Raf	5CSW	in	closed	out	RS3→	T	I ½A	F, G, B, FP-II, BP-I-A, BP-I-B, BP-II-in, BP-II-A-in
Dasatinib-Lyn[g]	2ZVA	in	open	in	RS2/3/4 up	T	I ½A	F, G, B, BP-I-A/B
Lapatinib-EGFR	1XKK	in	closed	out	RS2/3→	T	I ½A	F, G, B, BP-I-A/B, II in, IIA in
Lenvatinib-VEGFR	3WZD	in	?	in	RS3/4 up	V	I ½A	F, G, B, IB, II in
Vemurafenib-B-Raf	3OG7	in	?	out	RS3→	T	I ½A	F, G, B
Abemaciclib-CDK6	5L2S	in	?	out	RS3→	F	I ½B	F, FP-II
Alectinib-ALK	3AOX	in	closed	in	active	L	I ½B	F, FP-I
Ceritinib-ALK	4MKC	in	closed	in	active	L	I ½B	F, FP-I
Crizotinib-ALK	2XP2	in	closed	in	active	L	I ½B	F, FP-I
Crizotinib-Met	2WGJ	in	closed	out	←RS4	L	I ½B	F, FP-I
Erlotinib-EGFR	4HJO	in	closed	out	RS2/3→	T	I ½B	F, G, BP-I-A/B
Sunitinib- CDK2	3TI1	in	closed	out	RS3→	F	I ½B	F
Axitinib-VEGFR	4AG8	out	closed	in	←RS2/4	V	IIA	F, G, B, BP-I-B, II out
Imatinib-Abl[g]	1IEP	out	closed	in	←RS2	T	IIA	F, G, B, BP-I-A/B, II out, IV
Imatinib-Kit	1T46	out	closed	in	←RS2	T	IIA	F, G, B, BP-I-A/B, II out, IV
Nilotinib-Abl	3CS9	out	closed	in	←RS2	T	IIA	F, G, B, BP-I-A/B, II out, III, V
Ponatinib-Abl[g]	3OXZ	out	closed	in	←RS2	T	IIA	F, G, B, BP-I-A/B, II out, III, IV
Ponatinib-Kit	4U0I	out	closed	in	←RS2	T	IIA	F, G, B, BP-I-A/B, II out, III, IV
Ponatinib-B-Raf	1UWH	out	?	in	←RS2/4	T	IIA	F, G, B, BP-I-B, II out, III
Sorafenib-CDK8	3RGF	out	?	in	←RS2/4	F	IIA	F, G, B, BP-I-B, II out, III
Sorafenib-VEGFR	4ASD	out	closed	in	←RS2	V	IIA	F, G, B, BP-I-B, II-out, III
Bosutinib-Abl	3UE4	out	open	in	←RS2	T	IIB	F, G, BP-I-A/B
Nintedanib-VEGFR2	3C7Q	out	closed	in	←RS2	V	IIB	F, G, BP-I-B
Sunitinib-Kit	3G0E	out	closed	in	←RS2	T	IIB	F
Sunitinib-VEGFR	4AGD	out	closed	in	←RS2	V	IIB	F, BP-I-B
Cobimetanib-MEK1	4AN2	in	closed	out	RS3→	M	III	F,G, B, BP-II-in
Trametinib-MEK1	Model[h]	in	closed	out	RS3→	M	III	F,G, B, BP-II-in[e]
Afatinib-EGFR	4G5J	in	open	in	active	T	VI	F, G, BP-I-A/B
Ibrutinib-BTK	Model[i]	in	closed	in	inactive	T	VI	F, G, B, BP-I-A/B[e]

[a] All human proteins unless otherwise noted.
[b] Activation segment.
[c] Gatekeeper residue.
[d] F, front cleft; G, gate area; B, back cleft; from http://klifs.vu-compmedchem.nl/unless otherwise noted.
[e] Inferred.
[f] Chicken enzyme.
[g] Mouse enzyme.
[h] Ref. [47].
[i] Ref. [44].

Table 8
RET point mutations[a].

Mutations in the extracellular cysteine-rich segment	Protein kinase domain mutations	
Mutation	Mutation	Location
Exon 8 G533C	*Exon 13* E768D	Fourth residue of the αC-helix
Exon 10 C609F/G/R/S/Y	*Exon 13* L790F (RS4)	Beginning of the β4-strand
Exon 10 C611F/G/S/Y/W	*Exon 13* Y791F	Second residue of the β4-strand
Exon 10 C618F/R/S	*Exon 14* V804M/L (Sh2)	Gatekeeper residue
Exon 10 C620F/R/S	*Exon 14* Y806C	Hinge residue
Exon 11 C630R/Y	*Exon 15* A883F	Last residue of the β7-strand
Exon 11 D631Y	*Exon 15* S891A	Between β8-strand and activation segment
Exon 11 C634/F/G/R/W/Y	*Exon 16* M918T	End of the activation segment
Exon 11 K666E		

[a] Data from Ref. [24].

multikinase inhibitors that have been approved for other indications (www.brimr.org/PKI/PKIs.htm).

The leading hypothesis to explain the modest response of these multikinase inhibitors is related to the concomitant inhibition of VEGFR2, which limits the permissible dosage [24]. For example, at clinically achievable concentrations, cabozantinib and vandetanib are more effective inhibitors of VEGFR2 than of RET. In the case of cabozantinib, its IC_{50} value for VEGFR2 is 0.035 nM vs. 5.2 nM against RET, which is nearly 150 times as large [72]. None of the drugs listed in Table 6 were designed primarily as RET antagonists. Development of antagonists that target RET specifically may improve the effectiveness in the treatment of RET-driven cancers. BLU-667 and LOXO-292, two RET specific antagonists, are in the early developmental phase and have entered clinical trials for both thyroid and lung cancers (www.clinicaltrials.gov) [24].

Li et al. reported that RXDX-105 (CEP-32496), which was initially developed as a B-Raf inhibitor, exhibits an 800-fold selectivity toward RET vs. VEGFR2 (0.33 vs. 258 nM IC_{50} values) [73]. Based upon modeling studies, they reported that RXDX-105 binds to the DFG-D_{out} conformation and is classified as a type II RET inhibitor. This drug is in clinical trials in patients with advanced lung cancer and other solid tumors (www.clinicaltrials.gov). See Ref. [60] for a summary of the development of other RET inhibitors.

The estimated incidence of new cases associated with *RET* mutations or RET-fusion proteins in the United States is about 10,000 per year (Table 3). This is about the same as number of new cases of chronic myelogenous leukemia for which imatinib and second and third generation of BCR-Abl non-receptor protein-tyrosine kinase antagonists have proven clinically efficacious and commercially successful [33]. Accordingly, such findings suggest that the search for specific antagonists targeting RET-driven neoplasms is worthwhile.

In addition to the inhibition of wild type RET, studies have been performed on the ability of antagonists to inhibit RET mutants that occur in sporadic and familial medullary thyroid carcinomas and multiple endocrine neoplasia type 2 syndromes [24]. For example, alectinib is a good inhibitor of the RET M918T, V804L, or Y791 mutants, ponatinib is effective against the RET V804M gatekeeper mutant, and sunitinib is effective against the V804L gatekeeper mutant. Moreover, cabozantinib is an effective inhibitor of the RET M918T mutant, vandetanib is a good inhibitor of the RET C634W and M918T mutants while sorafenib is a potent antagonist of the RET C634R and M918T mutants. In contrast, lenvatinib is ineffective against the more common RET mutants.

As noted by Winer and colleagues "Biologically, the cancer cell is notoriously wily; each time we throw an obstacle in its path, it finds an alternate route that must then be blocked" [74]. Acquired resistance to RET antagonists occurs, but little is known about the resistance mechanisms. To date, no mutations have been reported in tumor samples from patients who have developed acquired resistance to these multikinase inhibitors [24]. The activation of bypass pathways is a likely mechanism for the development of some cases of acquired resistance following RET multikinase inhibitor treatment [75].

8. Epilogue

Manning et al. reported that the human protein kinase lineage consists of 518 members that include 478 typical and 40 atypical enzymes [5]. Based upon the identity of the phosphorylated —OH group, these enzymes are classified as protein-serine/threonine kinases (385 members), protein-tyrosine kinases (90), and protein-tyrosine kinase like enzymes (43). The protein-tyrosine kinases include both non-receptor (32) and receptor (58) proteins. A small group of enzymes such as MEK1/2, which catalyze the phosphorylation of both threonine and tyrosine residues within the activation segment of target proteins, are classified as dual specificity kinases. Although RET is only distantly related to MEK1/2, Plaza-Menacho reported that RET is a dual specificity kinase with the ability to catalyze the phosphorylation of both tyrosyl and seryl residues [9]. Furthermore, Plaza-Menacho described an active structure of RET with an open glycine-rich loop and an inactive structure of RET with a closed glycine-rich loop that is unable to bind ATP [7]. This finding adds another parameter in addition to the conformation of the αC-helix, the activation segment, and the regulatory spine in determining the differences between active and dormant protein kinases. RET is also an unusual receptor protein-tyrosine kinase owing to the requirement of GDNF family receptor-α co-receptors necessary for ligand-mediated activation.

Dysregulation of protein kinases plays a fundamental role in the pathogenesis of human illness, including autoimmune, cancer, inflammatory, and nervous system disorders. Accordingly, this family of enzymes has become one of the most important drug targets over the past two decades [59,76]. There are currently more than 250 protein kinase antagonists in various stages of clinical development worldwide. The 36 FDA-approved drugs target about 20 different protein kinases within the family with 518 members (www.brimr.org/PKI/PKIs.htm). Most of these approved drugs are used for the treatment of neoplastic disorders. Owing to their role in many aspects of cellular signaling, a much wider range of diseases should be amenable to treatments with protein kinase antagonists [77]. Accordingly, we can expect future advances in clinical effectiveness and the subsequent approval of additional drugs targeting (i) more protein kinases and (ii) other illnesses such as hypertension and Parkinson disease [76].

Conflict of interest

The authors are unaware of any affiliations, memberships, or financial holdings that might be perceived as affecting the objectivity of this review.

Acknowledgments

The colored figures in this paper were checked to ensure that their perception was accurately conveyed to colorblind readers [78]. The authors thank Laura M. Roskoski for providing editorial and bibliographic assistance. We also thank Josie Rudnicki and Jasper Martinsek help in preparing the figures and Pasha Brezina and W.S. Sheppard for their help in structural analyses.

References

[1] L.M. Mulligan, RET revisited: expanding the oncogenic portfolio, Nat. Rev. Cancer 14 (2014) 173–186.
[2] M. Takahashi, J. Ritz, G.M. Cooper, Activation of a novel human transforming gene, ret, by DNA rearrangement, Cell 42 (1985) 581–588.
[3] Y. Ishizaka, F. Itoh, T. Tahira, I. Ikeda, T. Sugimura, J. Tucker, et al., Human ret proto-oncogene mapped to chromosome 10q11.2, Oncogene 4 (1989) 1519–1521.
[4] P. Durbee, C.V. Marcos-Gutierrez, C. Kilkenny, M. Grigoriou, K. Wartiowaara, P. Suvanto, et al., GDNF signalling through the Ret receptor tyrosine kinase, Nature 381 (1996) 789–793.
[5] G. Manning, D.B. Whyte, R. Martinez, T. Hunter, S. Sudarsanam, The protein kinase complement of the human genome, Science 298 (2002) 1912–1934.
[6] M.A. Lemmon, J. Schlessinger, Cell signaling by receptor tyrosine kinases, Cell 141 (2010) 1117–1134.
[7] I. Plaza-Menacho, K. Barnouin, K. Goodman, R.J. Martínez-Torres, A. Borg, J. Murray-Rust, et al., Oncogenic RET kinase domain mutations perturb the autophosphorylation trajectory by enhancing substrate presentation in *trans*, Mol. Cell 53 (2014) 738–751.
[8] I. Plaza-Menacho, L. Mologni, N.Q. McDonald, Mechanisms of RET signaling in cancer: current and future implications for targeted therapy, Cell. Signal. 26 (2014) 1743–1752.

[9] I. Plaza-Menacho, K. Barnouin, R. Barry, A. Borg, M. Orme, R. Chauhan, et al., RET functions as a dual-specificity kinase that requires allosteric inputs from juxtamembrane elements, Cell Rep. 17 (2016) 3319–3332.
[10] X. Liu, Q.C. Vega, R.A. Decker, A. Pandey, C.A. Worby, J.E. Dixon, Oncogenic RET receptors display different autophosphorylation sites and substrate binding specificities, J. Biol. Chem. 271 (1996) 5309–5312.
[11] P.P. Knowles, J. Murray-Rust, S. Kjaer, R.P. Scott, S. Hanrahan, M. Santoro, et al., Structure and chemical inhibition of the RET tyrosine kinase domain, J. Biol. Chem. 281 (2006) 33577–33587.
[12] Y. Kawamoto, K. Takeda, Y. Okuno, Y. Yamakawa, Y. Ito, R. Taguchi, et al., Identification of RET autophosphorylation sites by mass spectrometry, J. Biol. Chem. 279 (2004) 14213–14224.
[13] J. Anders, S. Kjar, C.F. Ibáñez, Molecular modeling of the extracellular domain of the RET receptor tyrosine kinase reveals multiple cadherin-like domains and a calcium-binding site, J. Biol. Chem. 276 (2001) 35808–35817.
[14] R.L. Siegel, K.D. Miller, A. Jemal, Cancer Statistics, 2017, CA Cancer J. Clin. 67 (2017) 7–30.
[15] L. Kwatampora, S.P. Weitzman, M.A. Habra, N.L. Busaidy, Endocrine malignancies, in: H.M. Kantarjian, R.A. Wolff (Eds.), The MD Anderson Manual of Medical Oncology, third ed., McGraw-Hill Education, New York, 2016, pp. 903–932.
[16] J.A. Fagin, S.A. Wells Jr., Biologic and clinical perspectives on thyroid cancer, N. Engl. J. Med. 375 (2016) 1054–1067.
[17] J.F. Gainor, A.T. Shaw, Novel targets in non-small cell lung cancer: ROS1 and RET fusions, Oncologist 18 (2013) 865–875.
[18] A.T. Shaw, P.P. Hsu, M.M. Awad, J.A. Engelman, Tyrosine kinase gene rearrangements in epithelial malignancies, Nat. Rev. Cancer 13 (2013) 772–787.
[19] G.W. Krampitz, J.A. Norton, RET gene mutations (genotype and phenotype) of multiple endocrine neoplasia type 2 and familial medullary thyroid carcinoma, Cancer 120 (2014) 1920–1931.
[20] C. Romei, R. Ciampi, R. Elisei, A comprehensive overview of the role of the RET proto-oncogene in thyroid carcinoma, Nat. Rev. Endocrinol. 12 (2016) 192–202.
[21] H. Donis-Keller, S. Dou, D. Chi, K.M. Carlson, K. Toshima, T.C. Lairmore, et al., Mutations in the RET proto-oncogene are associated with MEN 2A and FMTC, Hum. Mol. Genet. 2 (1993) 851–856.
[22] R.M. Hofstra, R.M. Landsvater, I. Ceccherini, R.P. Stulp, T. Stelwagen, Y. Luo, et al., A mutation in the RET proto-oncogene associated with multiple endocrine neoplasia type 2B and sporadic medullary thyroid carcinoma, Nature 367 (1994) 375–376.
[23] L.M. Mulligan, J.B. Kwok, C.S. Healey, M.J. Elsdon, C. Eng, E. Gardner, et al., Germ-line mutations of the RET proto-oncogene in multiple endocrine neoplasia type 2A, Nature 363 (1993) 458–460.
[24] A. Drilon, Z.I. Hu, G.G.Y. Lai, D.S.W. Tan, Targeting RET-driven cancers: lessons from evolving preclinical and clinical landscapes, Nat. Rev. Clin. Oncol. (2017), http://dx.doi.org/10.1038/nrclinonc.2017.188 (Epub ahead of print).
[25] M. Grieco, M. Santoro, M.T. Berlingieri, R.M. Melillo, R. Donghi, I. Bongarzone, et al., PTC is a novel rearranged form of the *ret* proto-oncogene and is frequently detected in vivo in human thyroid papillary carcinomas, Cell 60 (1990) 557–563.
[26] T. Kohno, H. Ichikawa, Y. Totoki, K. Yasuda, M. Hiramoto, T. Nammo, et al., KIF5B-RET fusions in lung adenocarcinoma, Nat. Med. 18 (2012) 375–377.
[27] D. Lipson, M. Capelletti, R. Yelensky, G. Otto, A. Parker, M. Jarosz, et al., Identification of new ALK and RET gene fusions from colorectal and lung cancer biopsies, Nat. Med. 18 (2012) 382–384.
[28] A.M. Schram, M.T. Chang, P. Jonsson, A. Drilon, Fusions in solid tumours: diagnostic strategies, targeted therapy, and acquired resistance, Nat. Rev. Clin. Oncol. 14 (2017) 735–748.
[29] R. Roskoski Jr., Anaplastic lymphoma kinase (ALK) in the treatment of ALK-driven lung cancers, Pharmacol. Res. 117 (2017) 343–356.
[30] S.K. Hanks, T. Hunter, Protein kinases 6: The eukaryotic protein kinase superfamily: kinase (catalytic) domain structure and classification, FASEB J. 9 (1995) 576–596.
[31] D.R. Knighton, J.H. Zheng, L.F. Ten Eyck, V.A. Ashford, N.H. Xuong, S.S. Taylor, et al., Crystal structure of the catalytic subunit of cyclic adenosine monophosphate-dependent protein kinase, Science 253 (1991) 407–414.
[32] D.R. Knighton, J.H. Zheng, L.F. Ten Eyck, N.H. Xuong, S.S. Taylor, J.M. Sowadski, Structure of a peptide inhibitor bound to the catalytic subunit of cyclic adenosine monophosphate-dependent protein kinase, Science 253 (1991) 414–420.
[33] R. Roskoski Jr., A historical overview of protein kinases and their targeted small molecule inhibitors, Pharmacol. Res. 100 (2015) 1–23.
[34] D. Bajusz, G.G. Ferenczy, G.M. Keser, Structure-based virtual screening approaches in kinase-directed drug discovery, Curr. Top. Med. Chem. 17 (2017) 2235–2259.
[35] R. Roskoski Jr., Src protein-tyrosine kinase structure, mechanism, and small molecule inhibitors, Pharmacol. Res. 94 (2015) 9–25.
[36] S.S. Taylor, M.M. Keshwani, J.M. Steichen, A.P. Kornev, Evolution of the eukaryotic protein kinases as dynamic molecular switches, Philos. Trans. R Soc. Lond. B Biol. Sci. 367 (2012) 2517–2528.
[37] B. Nolen, S. Taylor, G. Ghosh, Regulation of protein kinases; controlling activity through activation segment conformation, Mol. Cell 15 (2004) 661–675.
[38] R. Roskoski Jr., ErbB/HER protein-tyrosine kinases: structures and small molecule inhibitors, Pharmacol. Res. 79 (2014) 34–74.
[39] R. Roskoski Jr., MEK1/2 dual-specificity protein kinases: structure and regulation, Biochem. Biophys. Res. Commun. 417 (2012) 5–10.
[40] J. Zhou, J.A. Adams, Participation of ADP dissociation in the rate-determining step in cAMP-dependent protein kinase, Biochemistry 36 (1997) 15733–15738.
[41] A.P. Kornev, N.M. Haste, S.S. Taylor, L.F. Ten Eyck, Surface comparison of active and inactive protein kinases identifies a conserved activation mechanism, Proc. Natl. Acad. Sci. U. S. A. 103 (2006) 17783–17788.
[42] A.P. Kornev, S.S. Taylor, L.F. Ten Eyck, A helix scaffold for the assembly of active protein kinases, Proc. Natl. Acad. Sci. U. S. A. 105 (2008) 14377–14382.
[43] R. Roskoski Jr., Anaplastic lymphoma kinase (ALK): structure, oncogenic activation, and pharmacological inhibition, Pharmacol. Res. 69 (2013) 69–94.
[44] R. Roskoski Jr., Ibrutinib inhibition of Bruton protein-tyrosine kinase (BTK) in the treatment of B cell neoplasms, Pharmacol. Res. 113 (2016) 395–408.
[45] R. Roskoski Jr., Cyclin-dependent protein kinase inhibitors including palbociclib as anticancer drugs, Pharmacol. Res. 111 (2016) 784–803.
[46] R. Roskoski Jr., ERK1/2 MAP kinases: structure, function, and regulation, Pharmacol. Res. 66 (2012) 105–143.
[47] R. Roskoski Jr., Allosteric MEK1/2 inhibitors including cobimetanib and trametinib in the treatment of cutaneous melanomas, Pharmacol. Res. 117 (2017) 20–31.
[48] R. Roskoski Jr., Janus kinase (JAK) inhibitors in the treatment of inflammatory and neoplastic diseases, Pharmacol. Res. 111 (2016) 784–803.
[49] R. Roskoski Jr., ROS1 protein-tyrosine kinase inhibitors in the treatment of ROS1 fusion protein-driven non-small cell lung cancers, Pharmacol. Res. 121 (2017) 202–212.
[50] R. Roskoski Jr., Vascular endothelial growth factor (VEGF) and VEGF receptor inhibitors in the treatment of renal cell carcinomas, Pharmacol. Res. 120 (2017) 116–132.
[51] H.S. Meharena, P. Chang, M.M. Keshwani, K. Oruganty, A.K. Nene, N. Kannan, et al., Deciphering the structural basis of eukaryotic protein kinase regulation, PLoS Biol. 11 (2013) e1001690.
[52] K. Shah, Y. Liu, C. Deirmengian, K.M. Shokat, Engineering unnatural nucleotide specificity for Rous sarcoma virus tyrosine kinase to uniquely label its direct substrates, Proc. Natl. Acad. Sci. U. S. A. 94 (1997) 3565–3570.
[53] Y. Liu, K. Shah, F. Yang, L. Witucki, K.M. Shokat, A molecular gate which controls unnatural ATP analogue recognition by the tyrosine kinase v-Src, Bioorg. Med. Chem. 6 (1998) 1219–1226.
[54] J.J. Liao, Molecular recognition of protein kinase binding pockets for design of potent and selective kinase inhibitors, J. Med. Chem. 50 (2007) 409–424.
[55] O.P. van Linden, A.J. Kooistra, R. Leurs, I.J. de Esch, C. de Graaf, KLIFS: a knowledge-based structural database to navigate kinase-ligand interaction space, J. Med. Chem. 57 (2014) 249–277.
[56] T. Kodama, T. Tsukaguchi, Y. Satoh, M. Yoshida, Y. Watanabe, O. Kondoh, et al., Alectinib shows potent antitumor activity against RET-rearranged non-small cell lung cancer, Mol. Cancer Ther. 13 (2014) 2910–2918.
[57] M. Song, Progress in discovery of KIF5B-RET kinase inhibitors for the treatment of non-small-cell lung cancer, J. Med. Chem. 58 (2015) 3672–3681.
[58] R. Roskoski Jr., Classification of small molecule protein kinase inhibitors based upon the structures of their drug-enzyme complexes, Pharmacol. Res. 103 (2016) 26–48.
[59] P.M. Fischer, Approved and experimental small-molecule oncology kinase inhibitor drugs: a mid-2016 overview, Med. Res. Rev. 37 (2017) 314–367.
[60] L. Mologni, C. Gambacorti-Passerini, P. Goekjian, L. Scapozza, RET kinase inhibitors: a review of recent patents (2012–2015), Expert Opin. Ther. Pat 27 (2017) 91–99.
[61] J. Krajewska, T. Gawlik, B. Jarzab, Advances in small molecule therapy for treating metastatic thyroid cancer, Expert Opin. Pharmacother. 18 (2017) 1049–1060.
[62] A.C. Dar, K.M. Shokat, The evolution of protein kinase inhibitors from antagonists to agonists of cellular signaling, Annu. Rev. Biochem 80 (2011) 769–795.
[63] J. Monod, J.P. Changeux, F. Jacob, Allosteric proteins and cellular control systems, J. Mol. Biol. 6 (1963) 306–329.
[64] F. Zuccotto, E. Ardini, E. Casale, M. Angiolini, Through the gatekeeper door: exploiting the active kinase conformation, J. Med. Chem. 53 (2010) 2691–2694.
[65] L.K. Gavrin, E. Saiah, Approaches to discover non-ATP site inhibitors, Med. Chem. Commun. 4 (2013) 41.
[66] V. Lamba, I. Ghosh, New directions in targeting protein kinases: focusing upon true allosteric and bivalent inhibitors, Curr. Pharm. Des. 18 (2012) 2936–2945.
[67] Z. Zhao, L. Xie, L. Xie, P.E. Bourne, Delineation of polypharmacology across the human structural kinome using a functional site interaction fingerprint approach, J. Med. Chem. 59 (2016) 4326–4341.
[68] W. Sherman, T. Day, M.P. Jacobson, R.A. Friesner, R. Farid, Novel procedure for modeling ligand/receptor induced fit effects, J. Med. Chem. 49 (2006) 534–553.
[69] C. Gao, M. Grøtli, L.A. Eriksson, Characterization of interactions and pharmacophore development for DFG-out inhibitors to RET tyrosine kinase, J. Mol. Model. 21 (2015) 167.
[70] R.A. Friesner, J.L. Banks, R.B. Murphy, T.A. Halgren, J.J. Klicic, D.T. Mainz, et al., Glide: a new approach for rapid, accurate docking and scoring: 1. Method and assessment of docking accuracy, J. Med. Chem. 47 (2004) 1739–1749.
[71] T.S. Gujral, V.K. Singh, Z. Jia, L.M. Mulligan, Molecular mechanisms of RET receptor-mediated oncogenesis in multiple endocrine neoplasia 2B, Cancer Res. 66 (2006) 10741–10749.

[72] F. Bentzien, M. Zuzow, N. Heald, A. Gibson, Y. Shi, L. Goon, et al., *In vitro* and *in vivo* activity of cabozantinib (XL184), an inhibitor of RET, MET, and VEGFR2, in a model of medullary thyroid cancer, Thyroid 23 (2013) 1569–1577.
[73] G.G. Li, R. Somwar, J. Joseph, R.S. Smith, T. Hayashi, L. Martin, et al., Antitumor activity of RXDX-105 in multiple cancer types with *RET* rearrangements or mutations, Clin. Cancer Res. 23 (2017) 2981–2990.
[74] E. Winer, J. Gralow, L. Diller, B. Karlan, P. Loehrer, L. Pierce, et al., Clinical cancer advances 2008: major research advances in cancer treatment, prevention, and screening–a report from the American Society of Clinical Oncology. J Clin Oncol 27:812-26. Erratum in, J. Clin. Oncol. 2009 (27) (2009) 3070–3071.
[75] M.J. Niederst, J.A. Engelman, Bypass mechanisms of resistance to receptor tyrosine kinase inhibition in lung cancer, Sci. Signal. 6 (294) (2013) re6.
[76] P. Cohen, D.R. Alessi, Kinase drug discovery –what's next in the field? ACS Chem. Biol. 8 (2013) 96–104.
[77] D.H. Drewry, C.I. Wells, D.M. Andrews, R. Angell, H. Al-Ali, A.D. Axtman, et al., Progress towards a public chemogenomic set for protein kinases and a call for contributions, PLoS One 12 (8) (2017) e0181585.
[78] R. Roskoski Jr., Guidelines for preparing color figures for everyone including the colorblind, Pharmacol. Res. 119 (2017) 240–241.